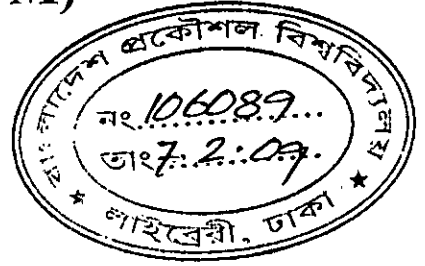


# Dynamic Characteristics of Servo-controlled Mobile Robot using Optimum Pulse Width Modulation (PWM)



by

**Muhammad Enayet Kabir**

MASTER OF SCIENCE IN MECHANICAL ENGINEERING

Department of Mechanical Engineering

BANGLADESH UNIVERSITY OF ENGINEERING AND TECHNOLOGY

DHAKA, BANGLADESH

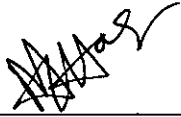





January 2009

## Certificate of Approval

The thesis titled "Dynamic Characteristics of Servo-controlled Mobile Robot using Optimum Pulse Width Modulation (PWM) by Muhammad Enayet Kabir , Roll No. 100610002P Session: October 2006 to the department of mechanical engineering of Bangladesh university of engineering and technology has been accepted as satisfactory for partial fulfillment of the requirements of the degree of Master of Science in Mechanical Engineering on 13 January 2009.

### BOARD OF EXAMINERS

1.   
\_\_\_\_\_  
Dr. Md. Zahurul Haq  
Professor  
Department of Mechanical Engineering  
BUET, Dhaka-1000  
(Supervisor) Chairman
2.   
\_\_\_\_\_  
Dr. M. A. Taher Ali  
Professor  
Department of Mechanical Engineering  
BUET, Dhaka-1000 Member
3.   
\_\_\_\_\_  
Dr. Abu Rayhan Md. Ali  
Professor and Head  
Department of Mechanical Engineering  
BUET, Dhaka-1000 Member  
(Ex-officio)
4.   
\_\_\_\_\_  
Professor Md. Abul Bashar  
Rtd. Director General  
Technical Education Member  
(External)

## Candidates Declaration

It is hereby declared that this thesis or any part of it has not been submitted elsewhere for the award of any degree or diploma.

Signature of the candidate

A handwritten signature in cursive script, appearing to read 'Muhammad Enayet Kabir', written above a dashed horizontal line.

Muhammad Enayet Kabir

# Table of Contents

List of Figure	v	
Acknowledgement	viii	
Abstract	ix	
<b>Chapter 1</b>	<b>Introduction</b>	
	1.1 Scope of the Study	1
	1.2 Scope of the Thesis	
<b>Chapter 2</b>	<b>Literature Review</b>	4
<b>Chapter 3</b>	<b>Design and Fabrication of Servo controlled Mobile Robot</b>	8
	3.1 Mechanical Structure and drive System	
	3.2 Robot Motion Control	10
	3.3 Robot Sensors	13
<b>Chapter 4</b>	<b>Data acquisition system</b>	16
		18
<b>Chapter 5</b>	<b>Results, Discussion and Conclusion</b>	24
	5.1.Result and Discussion	
	5.2. Conclusion	
	5.3 Scope of Further works	
References		49
Appendix A	Brief description of PIC 18 F 452	51
Appendix B	Brief description of PIC 18 F 2550	54
Appendix C	Brief description of MAX 232	59
Appendix D	USART Transmission and Receiving Block Diagrams	64

## List of Figures

Fig. No.	Title of the Figures	Page No.
Fig. 3.1.	Mobile robot with PC to acquire motion data and motor currents.	9
Fig. 3.2.	Circuit and wheels of the robot.	9
Fig. 3.3.	Two motors mounted on either side of the robot can power two wheels. Casters provide balance. The robot steers by changing the speed and direction of each motor.	11
Fig 3.4.	A robot with a front-drive motor mount uses a single opposing caster for balance. Steering is accomplished using the same technique as a centerline motor mount.	12
Fig. 3.5.	Basic H-bridge.	13
Fig. 3.5.	Basic H-bridge.	14
Fig. 3.7.	PWM signal and Duty cycle	15
Fig 3.8.	An optical shaft encoder attached to a motor, alternatively, a series of reflective strip on a black disk and LED light into the phototransistor can be placed.	17
Fig. 4.1.	Close up detail showing how synchronous serial data is only picked up on the clock edge.	19
Fig. 4.2.	Pin configuration of serial port, DB9	22
Fig. 5.1.	Motor traverse and the corresponding motor currents and battery voltage (unloaded motors with 100% duty cycle).	25
Fig. 5.2.	Motor traverse and the corresponding motor currents and battery voltage at the early stage of the motion (unloaded motors with 100% duty cycle).	25

Fig. 5.3.	Motor traverse and the corresponding motor currents and battery voltage at the final stage of the motion (unloaded motors with 100% duty cycle).	26
Fig. 5.4.	Motor traverse and the corresponding velocity (unloaded motors with 100% duty cycle).	27
Fig. 5.5.	Motor traverse and the corresponding acceleration (unloaded motors with 100% duty cycle).	27
Fig. 5.6.	Motor acceleration and the corresponding current (unloaded motors with 100% duty cycle).	28
Fig. 5.7.	Motor traverse and the corresponding motor currents and battery voltage (wheel load 13.5 Kg and motor PWM with 100% duty cycle).	29
Fig. 5.8.	Motor traverse and the motor currents and battery voltage at the early stage of the motion (wheel load 13.5 Kg and motor PWM with 100% duty cycle).	30
Fig. 5.9.	Motor traverse and the motor currents and battery voltage at the final stage of the motion (wheel load 13.5 Kg and motor PWM with 100% duty cycle).	30
Fig. 5.10.	Motor traverse and the corresponding velocity (wheel load 13.5 Kg and motor PWM with 100% duty cycle).	31
Fig. 5.11.	Motor traverse and the corresponding acceleration (wheel load 13.5 Kg and motor PWM with 100% duty cycle).	31
Fig. 5.12.	Motor traverse and the corresponding motor currents and battery voltage (wheel load 20.0 Kg and motor PWM with 100% duty cycle).	32
Fig. 5.13.	Motor traverse and the motor currents and battery voltage at the early stage of the motion (wheel load 20.0 Kg and motor PWM with 100% duty cycle).	33
Fig. 5.14.	Motor traverse and the motor currents and battery voltage at the final stage of the motion (wheel load 20.0 Kg and motor PWM with 100% duty cycle).	33
Fig. 5.15.	Motor traverse and the corresponding velocity (wheel load 20.0 Kg and motor PWM with 100% duty cycle).	34

Fig. 5.16.	Motor traverse and the corresponding acceleration (wheel load 20.0 Kg and motor PWM with 100% duty cycle).	34
Fig. 5.17.	Motor traverse and the corresponding velocity (unloaded motors with 100% duty cycle at right motor and 90% duty cycle at the left).	35
Fig. 5.18.	Motor traverse and the corresponding velocity (unloaded motors with 100% duty cycle at right motor and 85% duty cycle at the left).	36
Fig. 5.19.	Motor traverse and the corresponding motor currents and battery voltage (unloaded motors with 100% duty cycle at right motor, 85% at left motor).	36
Fig. 5.20.	Motor traverse and motor currents and battery voltage at the early stage of motion (unloaded motors, 100% duty cycle at right and 85% duty cycle at the left).	37
Fig. 5.21.	Motor traverse and motor currents and battery voltage at the final stage of motion (unloaded motors, 100% duty cycle at right and 85% duty cycle at the left).	37
Fig. 5.22.	Motor traverse and the corresponding velocity (unloaded motors with 100% duty cycle at right motor and 85% duty cycle at the left).	38
Fig. 5.23.	Motor traverse and the corresponding acceleration (unloaded motors with 100% duty cycle at right motor and 85% duty cycle at the left).	38
Fig. 5.24.	Motor traverse and motor currents and battery voltage (wheel load 13.5 Kg with 100% duty cycle at right motor and 85% duty cycle at the left).	39
Fig. 5.25.	Motor traverse, currents and battery voltage at the early stage of motion (wheel load 13.5 Kg, 100% duty cycle at right and 85% duty cycle at the left).	39
Fig. 5.26.	Motor traverse and currents and battery voltage at the final stage of motion (wheel load 13.5 Kg, 100% duty cycle at right motor and 85% duty cycle at the left).	40
Fig. 5.27.	Motor traverse and the corresponding velocity (wheel load 13.5 Kg with 100% duty cycle at right motor and 85% duty cycle at the left).	40

Fig. 5.28.	Motor traverse and the corresponding acceleration (wheel load 13.5 Kg with 100% duty cycle at right motor and 85% duty cycle at the left).	41
Fig. 5.29.	Motor traverse and motor currents and battery voltage (wheel load 20.0 Kg with 100% duty cycle at right motor and 85% duty cycle at the left).	41
Fig. 5.30.	Motor traverse and currents and battery voltage at early stage of motion (wheel load 20.0 Kg, 100% duty cycle at right and 85% duty cycle at the left).	42
Fig. 5.31.	Motor traverse and currents and battery voltage at the final stage of the motion (wheel load 20.0 Kg, 100% duty cycle at right and 85% duty cycle at left).	42
Fig. 5.32.	Motor traverse and the corresponding velocity (wheel load 20.0 Kg with 100% duty cycle at right motor and 85% duty cycle at the left).	43
Fig. 5.33.	Motor traverse and the corresponding acceleration (wheel load 20.0 Kg with 100% duty cycle at right motor and 85% duty cycle at the left).	43
Fig. 5.34.	Effect of load on motor traverse (100% duty cycle at right motor and 85% duty cycle at the left).	44
Fig. 5.35.	Effect of load on motor traverse at very early stage of motion (100% duty cycle at right motor and 85% duty cycle at the left).	45
Fig. 5.36.	Effect of load on motor speed (100% duty cycle at right motor and 85% duty cycle at the left)	45
Fig. 5.37.	Effect of load on motor current (100% duty cycle at right motor and 85% duty cycle at the left).	46
Fig. 5.38.	Effect of braking on motor traverse (100% duty cycle at right motor and 85% duty cycle at the left).	47



## **Acknowledgement**

I like to express my eternal gratitude to the thesis supervisor Dr. Md. Zahurul Haq, Professor, Department of Mechanical Engineering, BUET, Dhaka for his invaluable guidance, suggestions throughout the entire work.

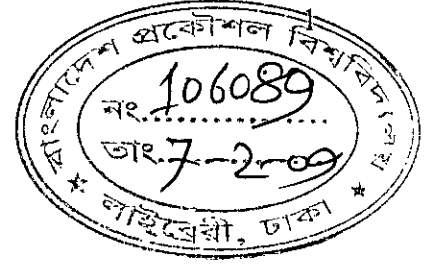
I also very thankful to Engineer, Mr. Ershed Zaman (Research Assistant), the personnel of Measurement, Instrumentation and Control Engineering Lab, Machine shop, carpentry shop and welding shop for their cooperation.

## **Abstract**

A mobile robot is designed and fabricated using locally available hardware components. It is driven by two independently controlled rear wheels and one un-powered omni-directional wheel in the front. A PIC microcontroller based system is used to take control actions using the feed-back signals. The response of the robot to the control actions is monitored using PC interfaced data acquisition system. Experimentations provided temporal motion data from wheels of the robot, motor currents and battery voltages. Data thus obtained is analyzed to obtain the response of the system to the control actions. When the drive motors are identically powered, it is found that the robot's left wheel motor is slightly faster than the right wheel motor. Experiments are carried out to find optimum duty cycle for the left motor to provide similar characteristics of the right motor. The optimum duty cycle thus obtained is verified at different loading conditions. Effect of loading on motor currents and robot dynamics is also analyzed and the effect of dynamic braking is found satisfactory.

# Chapter 1

## Introduction



The control of wheeled mobile robots has been, and still is, the subject of numerous research studies [1-5]. The rise in the popularity of the microcontroller and the drastic reduction in size and cost of integrated circuits in recent years have opened up new arenas for creating intelligent robotic systems [6]. Building a robot, however, requires more expertise than simple programming. Locomotion actuators, manipulators, control systems, sensor suits, efficient power supplies, well-engineered software—all of these subsystems have to be designed to fit together into an appropriate package suitable for carrying out the robot's task [8-10].

DC motors are comprehensively used in mobile robot applications [10-11]. These are driven directly by on-board battery; however, their speed characteristics are dependent on loading [7]. Even with identical motors powered from the same source, these exhibit variations in speed and torque to result in slightly curved motion. The variations in the motor characteristics and the friction in rotating components also contribute to this curved motion. Hence, feedback control using signal from a single wheel does not ensure straight motion, rather signals from two wheels have to be utilized [8]. The control action is usually in the form of the variation in the duty cycle of the pulse width modulation (PWM) control system [11]. However, very well defined strategy to estimate proper duty cycle is not available in the literature [1]. The matter is further complicated in case of acceleration, deceleration, braking and steering of the robots where duty cycle applied to the motors are varied to have desired motion characteristics.

Preliminary experimentation employed in Robocon 2005-2008 competition robots exhibited good responses as duty cycle is adjusted without proper analytical or systematic estimation. The present study focuses to have optimum parameters required to ensure desired motion as per required specification of speed and loading conditions.

## 1.1 Scope of the Study

Specific objectives of this study are as follows:

To design and fabricate an autonomous mobile robot using locally available hardware components.

To setup measuring instrumentation, drive actuators and control electronics.

To setup and fine-tune high speed sensor-PC interfacing system (developed for Robocon project) to acquire various motion characteristics i.e. acceleration, uniform speed cruise, deceleration, dynamic braking.

To analyze robot motion dynamics to obtain optimum PWM to ensure straight motion.

To analyze battery voltages and motor currents in response to robot motion and load variation.

In the present study, a mobile robot is designed and fabricated using locally available hardware components. The robot is driven by two independently controlled rear wheels and one un-powered omni-directional wheel in the front. Measuring instrumentation to provide feedback to the controller and speed encoders to send signals to the on-board PC is installed and tuned. A PIC microcontroller based system is used as the servo-controller to take control actions as per motion specification. Motion specification includes pre-specified acceleration, uniform speed cruise, deceleration and braking characteristics. The control action includes the variation of the duty cycle of pulse width modulation (PWM) to the relevant drive motor.

The response of the robot in response to the control actions is monitored and saved using high speed data acquisition system. Experimentations provide temporal motion data from wheels of the robot. Data thus obtained is analyzed to obtain the response of the system to the control actions. When the drive motors are powered at 100% duty cycle, it is found that the robot's left wheel motor is slightly faster than the right wheel motor which results in slightly curved path, probably because of their

variation in motor friction and characteristics. Experiments are carried out to find optimum duty cycle for the left motor to provide similar characteristics of the right motor. This optimum duty cycle of PWM is verified for the robot operation at different loading conditions. Effect of loading on motor currents and robot dynamics is also analyzed and the effect of dynamic braking is probed.

## **1.2 Scope of the Thesis**

The thesis reports the design and fabrication of a servo-controlled mobile robot using locally available hardware components. Here, the dynamics of the robot is also investigated. In this thesis, literature is reviewed in chapter 2. The design of the robot and its control mechanism is briefly presented in chapter 3. Data acquisition system to investigate the robot dynamics and motor currents is presented in chapter 4. Outcomes of the present works, conclusions of the thesis and the recommendations are presented in chapter 5.

# Chapter 2

## Literature Review

A robot is a machine designed to perform a broad variety of task and functions. Robots are often ideally suited for going where human being cannot go. Extremes of heat, cold, or nuclear radiation, and hostile environments such as war zones, the ocean deeps, or the surface of Mars, allow a well designed robot to operate where people will be unable to function, or would be killed [12].

Robots have been used in cleaning up environmental disaster sites such as the Chernobyl nuclear reactor. They are also used in mining exploration, land-mine detection, bomb disposal, and to attack enemy troops and vehicles. Teleoperated robots can be controlled by people from a remote location; autonomous robots can act on their own or cooperate with others. Given the wide variety of beneficial applications that people can develop for robots, the field of robotics has undergone tremendous growth in recent years; this growth will undoubtedly continue. Nevertheless, as the possible applications of robotics are expanded, some observers are concerned that these nonhuman “actors” may take on too much power and that people may not be able to control them [12].

What separates a robot from a simple machine is its versatility, flexibility, and adaptability. While a simple machine repeats a single task over and over, robots can usually be reprogrammed with new instructions to perform different tasks. Some robots also have the ability to “learn” and to reprogram themselves to accommodate changing situations [4].

All modern robots have a few features in common. The first is central processing unit that controls the robot and serves as its brain. This unit sends the commands that control the robot’s movements, interprets its sensor data, and communicates with humans. Computer programs control all of these actions. All robots also have some kind of body that can be almost any size or shape: Insectoid, vehicular, humanoid, and canine models are presently being made. In addition, there

must be some kind of interface—through the physical contact of wires or fiber-optic cables or the remote control of radio and microwave transmissions—through which people can communicate with the robot to extract its recorded data or send it new instructions. Finally, robots generally have a tool or sensor to manipulate or record data about an environment [8-10].

Robots typically have two methods of locomotion: wheels or legs. Robots with wheels or tank-like tracks are typically very stable on flat ground, but they quickly run into difficulties on uneven terrain, such as rocky landscapes or even a simple set of stairs. Legged robots can negotiate uneven terrain, but they are often extremely slow, and even more often have tremendous balance problems, even on relatively flat terrain. Working robots have been developed featuring all manner of locomotion, from a one-legged robot that must hop continuously to eight-legged spider-like models [13].

Robots can be made in almost any size. Today, feasible robots—from land rovers that measure a few centimeters to tanks and unmanned aircraft measuring tens of meters—are being produced or actively researched. They can be shaped into any mechanically feasible form. Robots' prime purposes are to accomplish a specific task, and they can easily be designed to carry and use any kind of tool. They can be equipped with guns, lasers, shovels, drill, video cameras, water cannons, radar, or scientific equipment. No robot carries all of these tools, of course; it would quickly become overly complicated and heavy [12].

Robots have three different degrees of independence [4]. At one extreme, tele-operated robots are controlled from a remote location by human beings who remain in constant communication with them [1,6]. At the other, autonomous robots are almost entirely independent of human control. They have almost complete independence in deciding how a task will be accomplished or a problem solved. In between, many robots combine properties of both independence and reliance on people. Tele-operated robots remain in contact with human controllers by radio contact or guide wires. These robots are typically used in strange environments where novel situations would befuddle an independent robot. The mobile robotic

rover Sojourner, of the 1997 Pathfinder mission to Mars, is an example of a tele-operated robot that was guided by earthbound humans. The robot was equipped to analyze Martian soil and rock samples. Ground controller on Earth chose the samples themselves. Autonomous robots are largely independent and must be carefully programmed to accomplish their goals. Simple tasks for a person, such as finding the way across a crowded room of moving people, are often complex and demanding tasks for an independent robot [12].

Robots are used for two principal reasons: to replace human labor for economic and or for safety purposes. The four major fields in which teleoperated and autonomous robots are used are industrial manufacturing, environmental cleanup, bomb disposal, and exploration of hostile environments. The U.S. government is the largest American user of robots for environmental cleanup.

Bomb disposal is the second-largest use of robotics. The robots used have the ability to examine suspicious packages and bombs with portable X-rays scanners to determine their contents and components. They are also equipped with manipulators to contain and sometimes inactivate the explosives. Robots are also being used in hostile and battlefield environments as security and defensive systems. Tele-operated tanks have already been developed for combat. Using these still requires a human operator, but one who can remain in safety hundreds of kilometers away. If the robot is destroyed, the operator can simply start up another robot, without loss of human life. Robot systems may someday be used by police to flush out fugitives and criminals from fortified positions.

The biggest problem with all robots is getting them to learn from experience. This is the prime problem faced by all artificial intelligence researchers [14]. Robots must somehow be programmed to learn from their mistakes, anticipate problems, and come up with novel solutions. Computer scientists try to make robots mimic human thought process, but since these aren't fully understood either, robots are still falling short of human ideals. Two well-understood methods of problem solving are the top-down and bottom-up methods.



A problem related to learning is co-evolution. This is when roboticist tries to get many robots to work together and cooperate at solving problems. Each robot—they can be the same or different models—can learn through trial and error and hopefully, specialize at performing a single task that will further the solution to the overall problem. For this to occur, each robot must be a flexible learner, able to cooperate with others, and perhaps give and receive orders. One example of the progress in creating successful cooperation among robots is the Robot World Cup, or Robo-cup and Robocon.

Since the introduction of machines, people have always worried about being replaced by mechanize labor. This fear is still with us today. Robots and other machines have encroached upon manual labor in all areas of human endeavor. Car factories use robots for assembly [2,5]. Computer Animation has replaced hand-painted animation cells, and Music Synthesizers mimic human musicians. Not all of these things are necessarily bad. Robots can perform dangerous tasks in a factory, and computers have opened up entirely new avenues of expression in the creative arts.

Industrial robotics now is being popularized that is the discipline concerning robot design, control and application in industry, and its products have by now reached the level of a mature technology [5]. The connotation of a robot for industrial application is that of operating in a structured environment whose geometrical or physical characteristics are mostly known a priori. However, mobile robotics is a rapidly developing branch of engineering [1-4].

## Chapter 3

### Design and Fabrication of Servo-controlled Mobile Robot

A robot is a special brew of motors, solenoids, wires, and assorted electronic odds and ends, a marriage of mechanical and electronic gizmos. Taken together, the parts make a half-living but wholly personable creature that can vacuum the floor, serve drinks, protect the family against intruders and fire, entertain, educate, and lots more. In the present research work, an autonomous mobile robot is designed and fabricated using locally available hardware components.

The designed robot is a three wheeler mobile robot with two independently controllable wheels at the rear and a free un-powered caster at the front. The front caster has omni directional capability and which is not controlled. Here, H-Bridge circuit is used to control the direction and driving of the two rear wheels. In-house encoders are attached to the rear wheels to provide feedback signals using IR transducers. The signal is then conditioned and communicated to the servo-controller (using PIC 18F452) and also to the data acquisition system (using PIC18F2550). The encoders generate 72 signals per rotation of wheel and each rotation of wheel generates 40 cm of linear motion. Robot motion is controlled by microcontroller using Pulse Width Modulation (PWM). The control action depends on the motion specification and the feed-back signals.

At first, the mechanical drive is designed and fabricated. After that control circuitry is attached with the drive unit. The robot components along with the data acquisition system is shown in Figs. 3.1 and 3.2. The robot has the following key components:

- Mechanical structure and drive unit.
- Motor control board having the relays and H-bridge.

- The microcontroller (PIC 18 F 452) board.
- Sensors and signal conditioners for sensors.

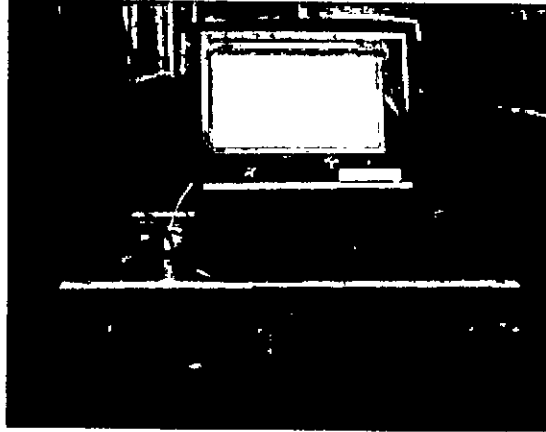


Fig. 3.1. Mobile robot with PC to acquire motion temporal data and motor currents.

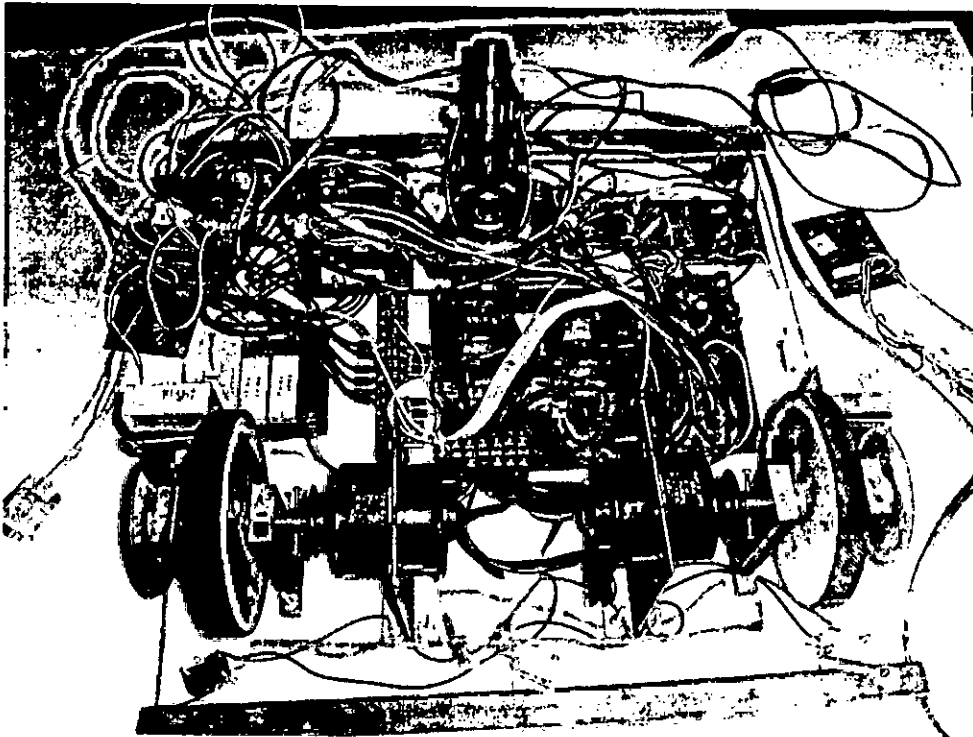


Fig. 3.2. Control and sensor circuits and the robot wheels.

### 3.1 Mechanical Structure and Drive System

The drive motors are probably the heaviest component in the robot and so as to the location of the drive motors are carefully considered. The weight is also distributed throughout the base. The mobile robot is designed using two identical motors to spin two wheels on opposite sides of the base (like the differentially driven robot). These wheels provide forward and backward locomotion, as shown in Fig. 3.3, as well as left and right steering. If the left motor is stopped, the robot turns to the left. By reversing the motors relative to one another, the robot turns by spinning on its wheel axis (turns in place). This forward reverse movement may also be used to make hard or sharp right and left turns.

For two wheels there are separate shafts and shafts are mounted using two ball bearings. The bearings are housed in the housing of mild steel. Two shafts are identical and aligned. The two wheels are made of plastic and coupled with the shafts. For counting the wheel rotation, the encoders are coupled with the shaft at the outer end. The base platform is made of plexy glass. It is a transparent and light-weight base for the robot upon which a laptop is placed to acquire data.

The designed robot is a three wheeler robot with two independently controllable wheels at the rear and a free un-powered caster at the front. The wheels are positioned and aligned between them. The caster on the other end is to provide stability and a pivot for turning. The robot has no “front” or “back,” at least as far as the drive system is concerned. Therefore, by using a caster in one end the robot became a kind of multidirectional robot that can move forward and backward with the same ease. Of course, this approach also complicates the bump sensors arrangement of the robot. Instead of having bump switches only in the front of the robot, additional bump switches are fixed in the back in case the robot is reversing the direction. One advantage of front-drive mounting is that it simplifies the construction of the robot.

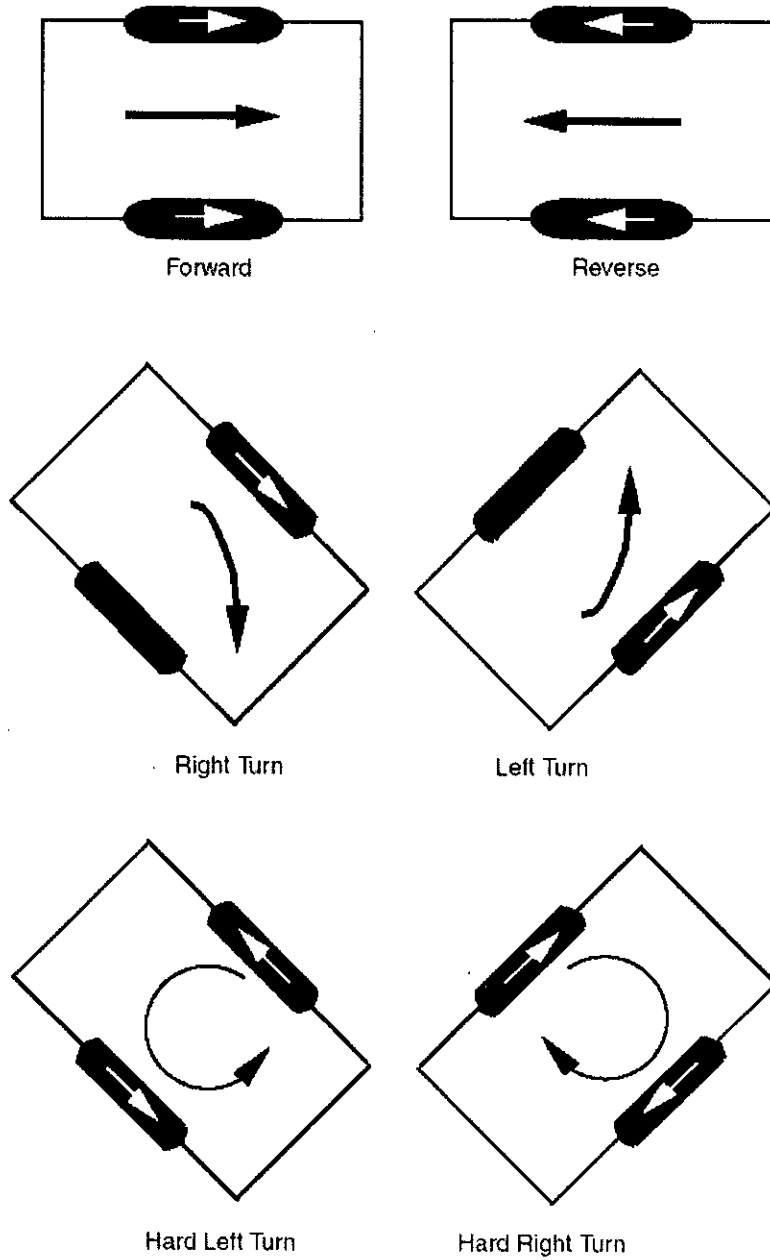


Fig. 3.3. Two motors mounted on either side of the robot can power two wheels. Casters provide balance. The robot steers by changing the speed and direction of each motor.

## Caster choices

For the right choice of caster the followings are normally considered:

- The size of the caster wheel should be in proportion to the drive wheels.
- When the robot is on the ground, the drive motors must firmly touch terra firma. If the caster wheels are too large, the drive motors may not make adequate contact, and poor traction will result. Use of a suspension system may also be considered on the casters to compensate for uneven terrain.
- The casters should spin and swivel freely. A caster that doesn't spin freely will impede the robot's movement. In most cases, since the caster is provided only for support and not traction, the caster should be constructed from a hard material to reduce friction. A caster made of soft rubber will introduce more friction, and it may affect a robot's movements.

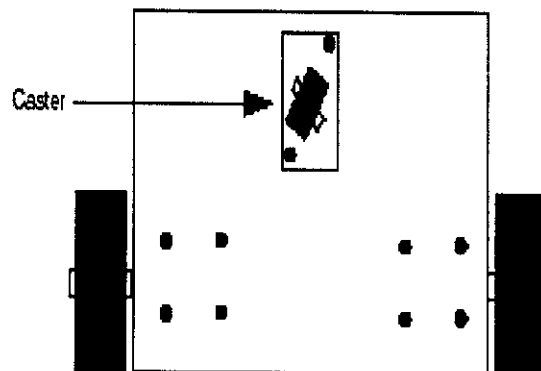


Fig 3.4. A robot with a front-drive motor mount uses a single opposing caster for balance. Steering is accomplished using the same technique as a centerline motor mount.

### 3.2 Robot Motion Control

In the robot, H-bridge Circuit is used to run the motor in different direction, as shown in Fig. 3.5. The basic operating mode of an H-bridge is fairly simple. In the diagram shown below is a simple H-bridge circuit to show the principle of H-bridge. Practical circuit consists of other components such as diodes for securing the circuit from other disturbance like back emf. In the H-bridge, there are 4 switches. In the circuit, the Single Pole, Double Through (SPDT) relay is used as switch. The coil of the relay is energized by ULN2803. To control the different direction of the motor two relays at a time are to be switched on. If upper left side relay and lower right side relay are turned on, the right lead of the motor will be connected to ground, while the left lead is connected to the power supply. Current starts flowing through the motor which energizes the motor in (let's say) the forward direction and the motor shaft starts spinning. If upper right side relay and lower left side Relay are turned on, the converse will happen, the motor gets energized in the reverse direction, and the shaft will start spinning in that way (Shown in Fig. 3.6). If less than full-speed (or torque) operation is intended one of the switches are controlled in a PWM fashion. The average voltage seen by the motor will be determined by the ratio between the 'on' and ' off time of the PWM signal.

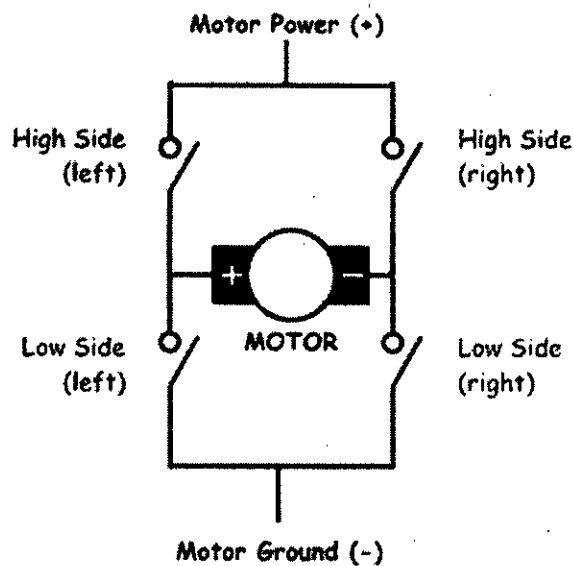


Fig. 3.5. Basic H-bridge.

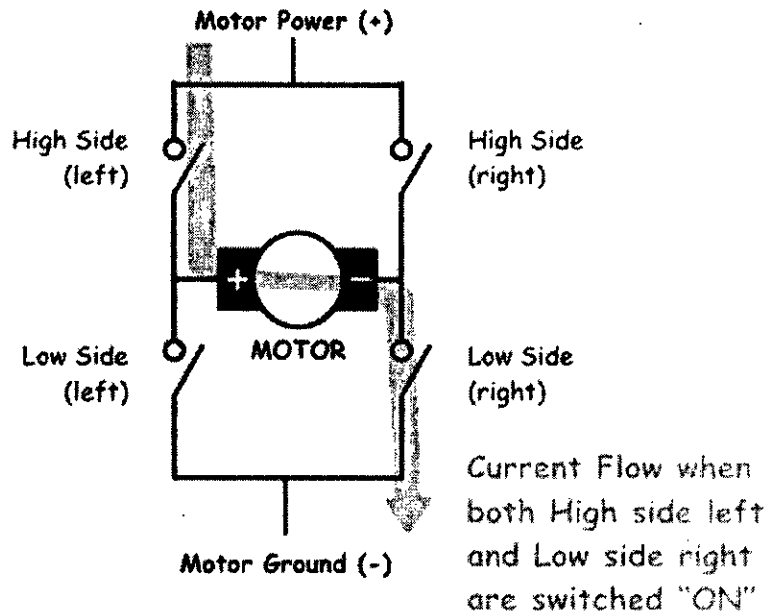


Fig. 3.6. Motor direction control using H-bridge.

### Pulse Width Modulation ( PWM )

To Control the Robot speed, PWM is used. Two PWMs are used to control the speeds of the two wheels. So by varying these two speeds, the direction of the robot can be changed. PWM is a way of digitally encoding analog signal levels. Through the use of high resolution counter, the duty cycle of a square wave is modulated to encode a specific analog signal level. The PWM signal is still digital because, at any given instant of time, the full DC supply is either fully on or fully off. The voltage or current source is supplied to the analog load by means of a repeating series of on and off pulses. The on-time is the time during which the DC supply is applied to the load, and the off-time is the period in which that supply is switched off. Given a sufficient bandwidth, any analog value can be encoded with PWM. Pulse-width modulation control works by switching the power supplied to the motor on and off very rapidly. The DC voltage is converted to a square-wave signal, alternating between fully on (nearly 5V or 12V) and zero, giving the motor a series of power "kicks". If the switching frequency is high enough (10kHz frequency is used in the present study), the motor runs at a steady speed due to its fly-wheel momentum. By adjusting the



duty cycle of the PWM i.e., the time fraction during which it is "on", the average power can be varied, and hence the motor speed (shown in Fig. 3.7).

One of the advantages of PWM is that the signal remains digital all the way from the processor to the controlled system; no digital-to-analog conversion is necessary. By keeping the signal digital, noise effects are minimized. Noise can only affect a digital signal if it is strong enough to change a logic-1 to a logic-0, or vice versa.

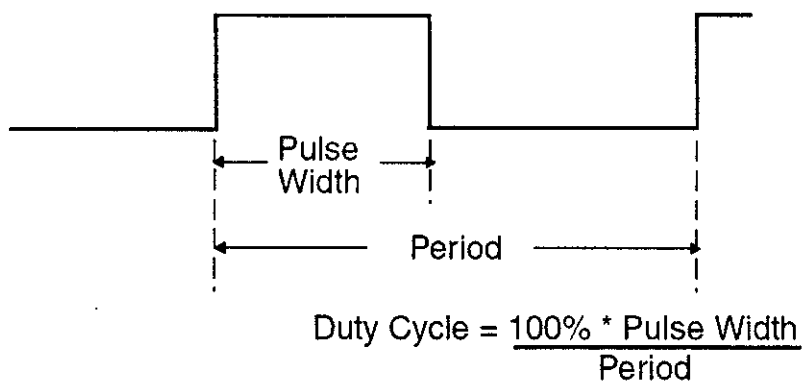


Fig. 3.7. PWM signal and Duty cycle

The H-bridge circuit and the duty cycle of PWM applied to the motors are set by the PIC18F452 microcontroller and a brief summary of its characteristics is presented in Appendix A.

### 3.3 Robot Sensors

The robot controller calculates the path movement with the help of shaft encoder. The materials for the completed shaft encoder consist of the encoder wheel, IR emitter/detector, black plastic film canister, and a cable tie. The wheel is attached to the rear of the motor shaft. The optical sensors are mounted on a small piece of board with a couple of other components. When the wheel attached at the rear side of the motor moves, it block the optical sensors emitter and receiver. By blocking like this, controller system can recognize this state. Thus the moving path can be

measured by counting these state positions. Infrared-sensitive phototransistor is positioned directly opposite the LED (see Fig. 3.8) so that when the motor and disc turn, the holes pass the light intermittently. The result, as seen by the phototransistor, is a series of flashing light. The number of slots in the disc determines the maximum accuracy of the travel circuit. The more slots the disc has, the better the accuracy. The encoder disc has 72 slots around its circumference, that represents a minimum sensing angle of  $5^\circ$  interval. As the wheel rotates, it provides a signal to the counting circuit every  $5^\circ$ . Stated another way, if the robot is outfitted with a 12.73 cm wheel (circumference 40cm), the maximum travel resolution is approximately 0.55 linear centimeter. This figure is calculated by taking the circumference of the wheel and dividing it by the number of slots in the shaft encoder. The outputs of the phototransistor are conditioned by Schmitt triggers. This smoothes out the wave shape of the light pulses so only voltage inputs above or below a specific threshold are accepted (this helps prevent spurious triggers). The output of the triggers is applied to the control circuitry of the robot.

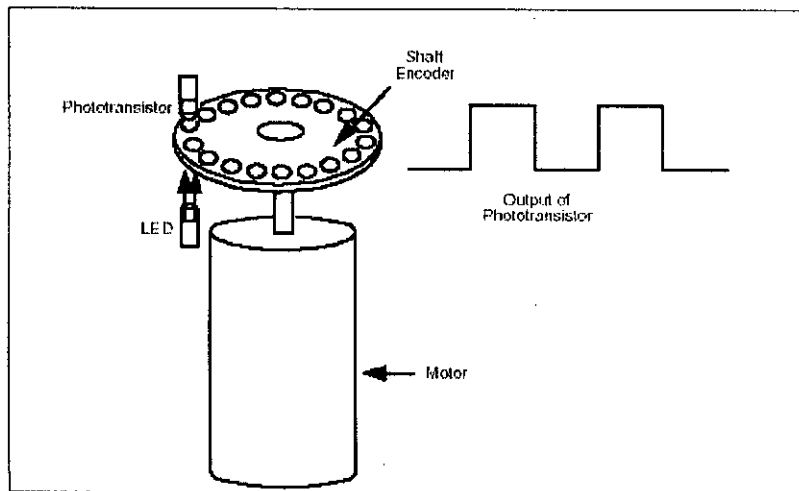


Fig 3.8. An optical shaft encoder attached to a motor, alternatively, a series of reflective strip on a black disk and LED light into the phototransistor can be placed.

**Microswitches**

Touch is a proactive event, by means of which the robot can determine its environment by making physical contact. Conversely, collision is a reactive event, where (in most cases) the robot is to stop what it's doing when a collision is detected and back away from the condition. One of the most convenient components used for sensing objects is the Micro-limit-switch. The micro-switch used in the robot has a double throw internal switch (three connections a common, a normally open, and a normally closed).

## **Chapter 4**

### **Data Acquisition System**

The basic input and output of a computer or microcontroller is a two-state binary voltage level (off and on), usually 0 and 5 V. For example, to place an output of a computer or microcontroller to high, the voltage on that output is brought, under software control, to 5 V. In addition to standard low/high inputs and outputs, there are several other forms of I/O found on single-board computers and microcontrollers.

In the present study, motor speed parameters are obtained using a PIC18F2550 based data acquisition system, developed under Robocon project. Brief introduction to PIC18F2550 is presented in Appendix B. Battery voltages and motor currents are also measured using ADC present in the microcontroller based measurement system. This microcontroller contains seven 10 bit ADC and therefore provides 0.01% accuracy. Data obtained in the present study is communicated to the onboard laptop computer using universal serial asynchronous communication (USART) and RS -232 interface, a detail of which is briefly presented in appendice C and D.

#### **Analog-To-Digital (ADC) Conversion**

Analog to digital conversion is used to measure battery voltages and the motor currents. This Analog-to-digital conversion (ADC) transforms analog (linear) voltage to binary (digital). In this project three ADC inputs are used, one for main battery voltage measurement and other two for two drive motor voltages. The output of the ADC is a number between 0 and 1023, and the number is directly related to the measured voltage.

## Serial Communications

The most common type of computer interfacing is known as serial, in which multiple bits are sent as a series of bits over time on a single wire. There are a number of different types of serial communications protocols, with asynchronous, synchronous, and Manchester encoding. Each methodology is optimized for different situations. The two most likely communications methods for interfacing a robot controller to I/O devices is synchronous serial communications, which consists of a data line and a clock line as shown in Fig. 4.1.

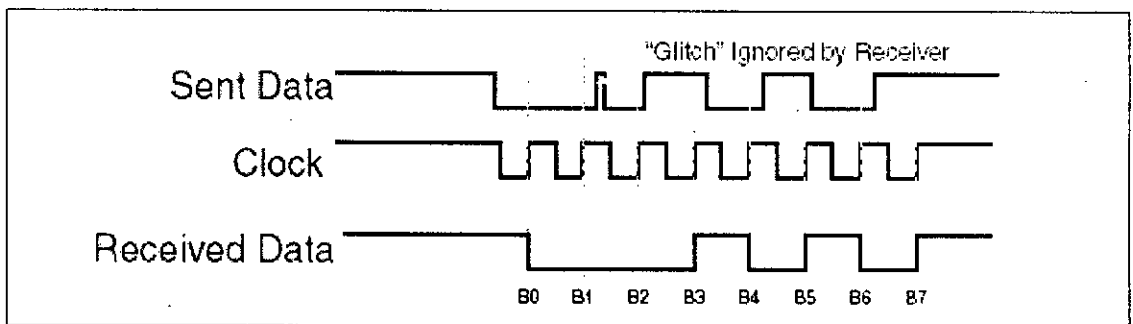


Fig. 4.1: Close up detail showing how synchronous serial data is only picked up on the clock edge.

## Asynchronous serial communications

Asynchronous serial communications uses a single wire to send a packet that consists of a number of bits, each the same length. The most popular data protocol for asynchronous serial communications is known as non-return to zero (NRZ) and consists of the first bit. The Start Bit is low and is used by the receiver to identify the middle of each bit of the incoming data stream for the most accurate reading as shown in Fig. 4.2. There can be any number of data bits, but for most communications, eight bits, allowing the transmission of a byte, are used. The following data bits have the same period and are read as they are received. The stop bit is a high value (the non-return to zero that resets the data line to a high value so the next start bit will be detected by the receiver) that provides a set amount of time for the sender and receiver to prepare for the next data packet. An error detection bit

can be placed at the end of the data bits, but this is rarely done in modern asynchronous serial communications. The most popular form of asynchronous serial communications is commonly referred to as RS-232 (although more accurately known as EIA-232) and changes the normal TTL voltage levels of the serial data from 0 to 5 V to 12 (0) and  $\bar{12}$  (1) V.

### **MAX232**

The Maxim MAX232, which generates the positive and negative voltages on the chip from the 5 V supply. Along with RS-232, RS-422, and RS-485 are commonly used forms of asynchronous serial communications, and like RS-232, these standards can be implemented using commonly available chips. Sending and receiving RS-232 data in a computer system may seem like a chore, but it is actually simplified by the universal asynchronous receiver/transmitter (known by its acronym UART) that will send and receive NRZ asynchronous data automatically with the computer system writing to it to start a data send or polling the UART to determine if the last written data byte has been sent or if data has been received. Along with the send and receive data bits, there are a number of other lines that can be used with RS-232 for handshaking (system-to-system communications to indicate that data can be sent or received) but these lines are largely ignored in most modern communications. The UART generally will provide an interface to these bits as well.

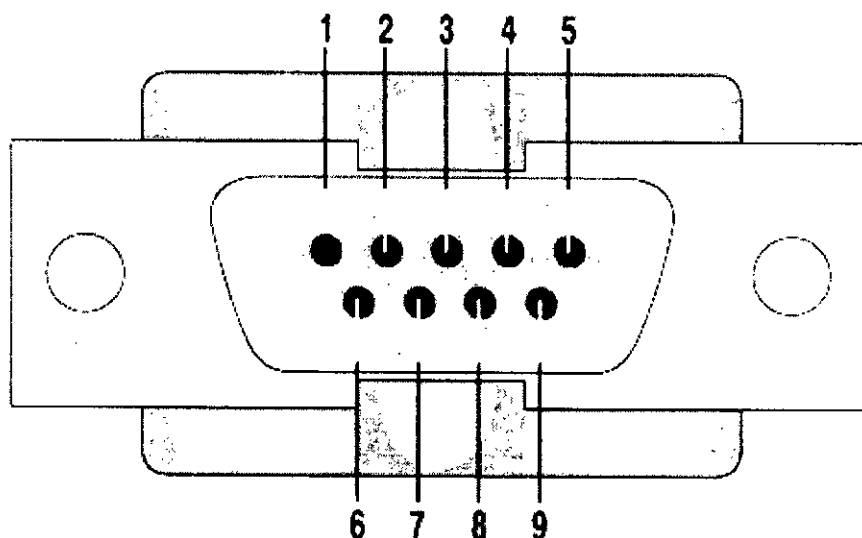
### **RS 232**

Electronic data communications between elements will generally fall into two broad categories: single-ended and differential. RS232 (single-ended) is introduced in 1962, and despite rumors for its early demise, has remained widely used through the industry. Independent channels are established for two-way (full-duplex) communications. The RS232 signals are represented by voltage levels with respect to a system common (power / logic ground). The "idle" state (MARK) has the signal level negative with respect to common, and the "active" state (SPACE) has the signal

level positive with respect to common. RS232 has numerous handshaking lines (primarily used with modems), and also specifies a communications protocol.

The RS-232 interface presupposes a common ground between the Data Terminal Equipment (DTE) and Data Communications Equipment (DCE). This is a reasonable assumption when a short cable connects the DTE to the DCE, but with longer lines and connections between devices that may be on different electrical busses with different grounds, this may not be true. RS232 data is bi-polar +3 to +12 volts indicate an "ON or 0-state (SPACE) condition" while A -3 to -12 volts indicates an "OFF" 1-state (MARK) condition. Modern computer equipment ignores the negative level and accepts a zero voltage level as the "OFF" state. In fact, the "ON" state may be achieved with lesser positive potential. This means circuits powered by 5 VDC are capable of driving RS232 circuits directly, however, the overall range that the RS232 signal may be transmitted/received may be dramatically reduced. The output signal level usually swings between +12V and -12V. The "dead area" between +3V and -3V is designed to absorb line noise. In the various RS-232-like definitions this dead area may vary. For instance, the definition for V.10 has a dead area from +0.3V to -0.3V. Many receivers designed for RS-232 are sensitive to differentials of 1 V or less.

Details of character format and transmission bit rate are controlled by the serial port hardware, often a single integrated circuit called a UART that converts data from parallel to asynchronous start-stop serial form. Details of voltage levels, slew rate, and short-circuit behavior are typically controlled by a line-driver that converts from the UART's logic levels to RS-232 compatible signal levels, and a receiver that converts from RS-232 compatible signal levels to the UART's logic levels.



Pin	Signal	Pin	Signal
1	Data Carrier Detect	6	Data Set Ready
2	Received Data	7	Request to Send
3	Transmitted Data	8	Clear to Send
4	Data Terminal Ready	9	Ring Indicator
5	Signal Ground		

Fig. 4.2. Pin configuration of serial port, DB9 used for RS -232 based serial data communication.

RS-232 devices may be classified as Data Terminal Equipment (DTE) or Data Communications Equipment (DCE); this defines at each device which wires will be sending and receiving each signal. The standard recommended but did not make mandatory the D-subminiature 25 pin connector. In general and according to the standard, terminals and computers have male connectors with DTE pin functions, and modems have female connectors with DCE pin functions. Other devices may



have any combination of connector gender and pin definitions. Many terminals are manufactured with female terminals but are sold with a cable with male connectors at each end; the terminal with its cable satisfied the recommendations in the standard. The standard specifies 20 different signal connections. Since most devices use only a few signals, smaller connectors can often be used. For example, the 9 pin DB-9 connector is used by most IBM-compatible PCs since the IBM PC AT, and has been standardized as TIA-574. In this data acquisition system DB-9 has been used.

# Chapter 5

## Results, Discussion and Conclusion

In the present study, experiments are carried out at different loading conditions with 100% duty cycle of applied pulse width modulation (PWM) to both the motors. Readings from the shaft encoders from the wheels are recorded at 4 ms intervals. Battery voltage and motor currents are also recorded. The robot's motions are found to be slightly curved as left motor moved faster, and therefore PWM of the motors are varied to obtain optimum value for straight robot motion. Various motion parameters are investigated and analyzed at different loading conditions.

### 5.1 Results and Discussion

Shown in Fig. 5.1 are the robot's motor traverse, battery voltage and the motor currents plotted as a function of time when the unloaded motors ran at 100% duty cycle. The motors traverses are increased with time, but the left motor moves faster. This results in slightly curved motion of the robot. At the very beginning, it is noticed that the motor currents increase very quickly and the rate is higher for the left motor, even before the motion has started. This current rush results in lowering of the battery voltage, as battery can't cope with the sudden demand of the current. The motors starts moving with slight delay of about 50 ms and the currents starts to decrease as shown in Fig. 5.2. The current falls as the result of the generation of the back emf that reduces effective voltage across the motor armature. With the decrease in the motor current, battery voltage starts to recover. It is seen, as shown in Figs. 5.1 and 5.3, that the motor currents are reduced to zero when a particular motor has traversed the set distance of 10 m, but no dynamic brake is applied. The distance of 10 m is used to take the readings due to the limitation of space availability. After both the motors traverse 10 m, dynamic brake is applied to both the motors and the robot moves slightly due to inertia action. In this case, there is no current demand for

the motors. Therefore, the battery voltage recovers more but it takes long time to recover to its “static voltage”.

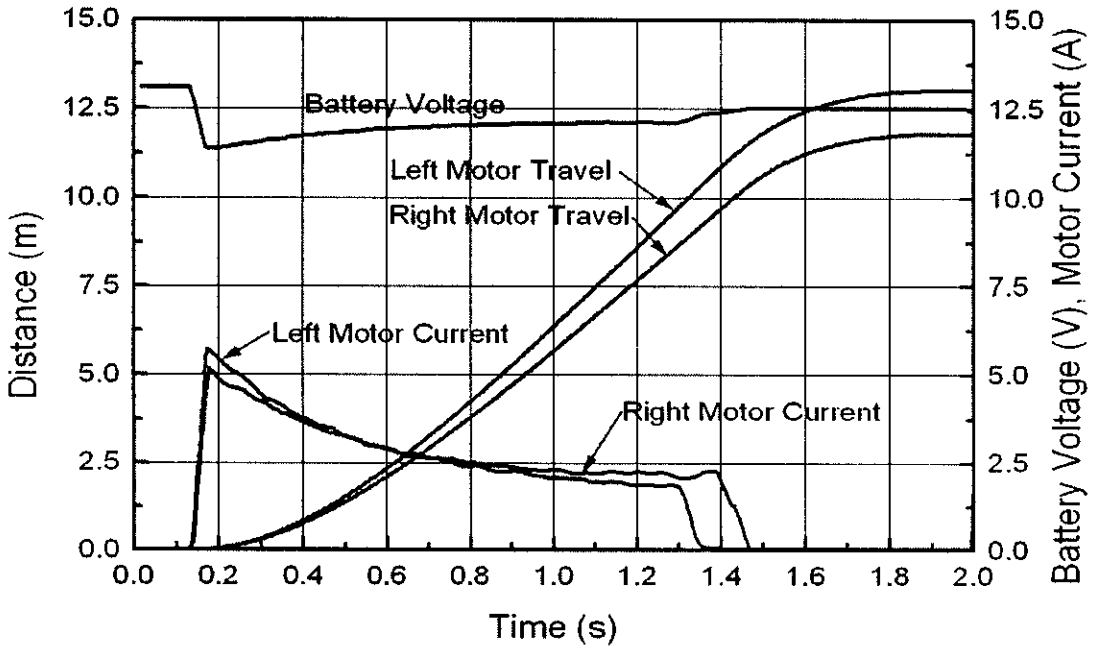


Fig. 5.1. Motor traverse and the corresponding motor currents and battery voltage (unloaded motors with 100% duty cycle).

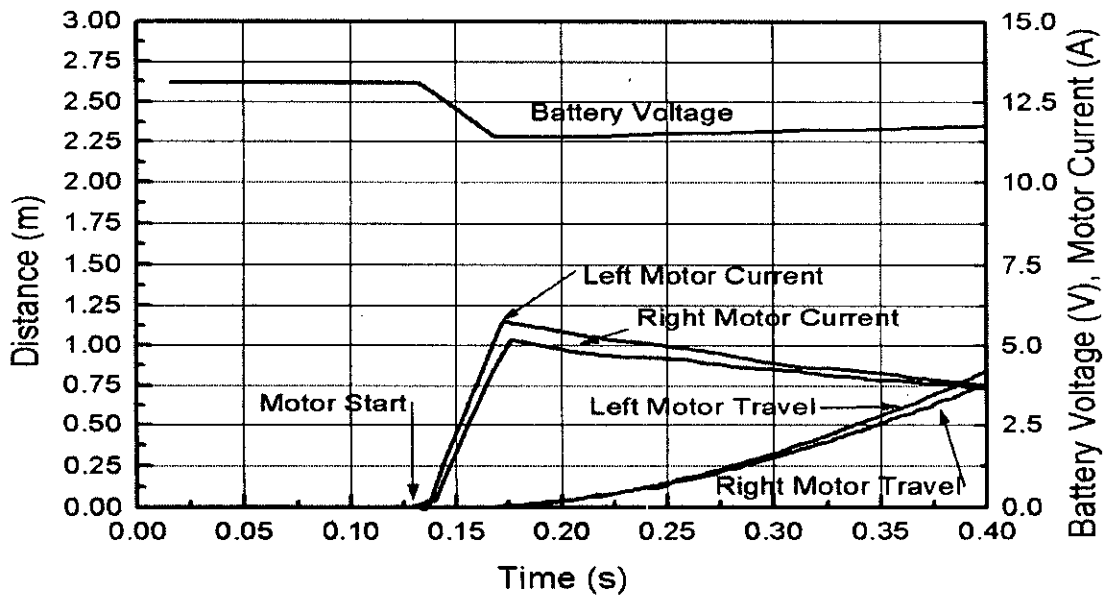


Fig. 5.2. Motor traverse and the corresponding motor currents and battery voltage at the early stage of the motion (unloaded motors with 100% duty cycle).

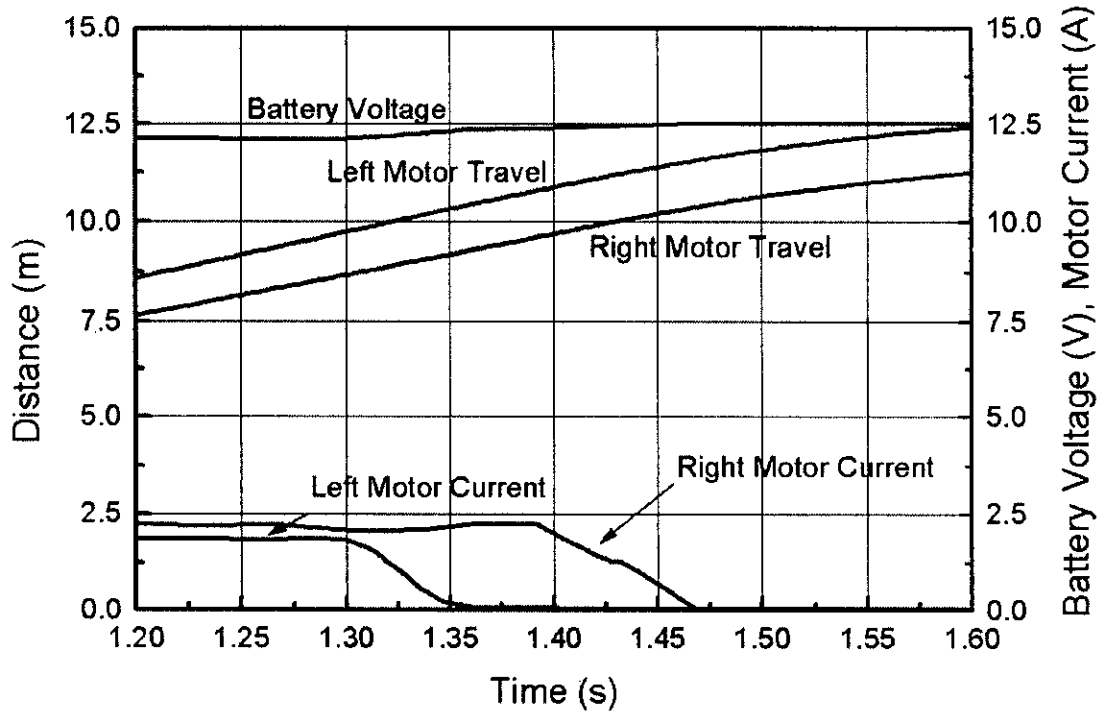


Fig. 5.3. Motor traverse and the corresponding motor currents and battery voltage at the final stage of the motion (unloaded motors with 100% duty cycle).

Shown in Figs. 5.4 and 5.6 are the motor velocity and the accelerations for the same conditions as shown in Figs. 5.1-5.3. The gradual increase in both the motors are clearly seen in Fig. 5.4, however, the left motor exhibit higher velocity. After reaching the set distance of 10 m, the duty cycle of PWM is reduced zero, so the left motor starts to slow down. Dynamic brakes are applied after the right motor crosses 10 m distance and there is reduction of velocity of both the motors. It may also be noted that at this stage the motors had same velocities and therefore the robot motion is straight.

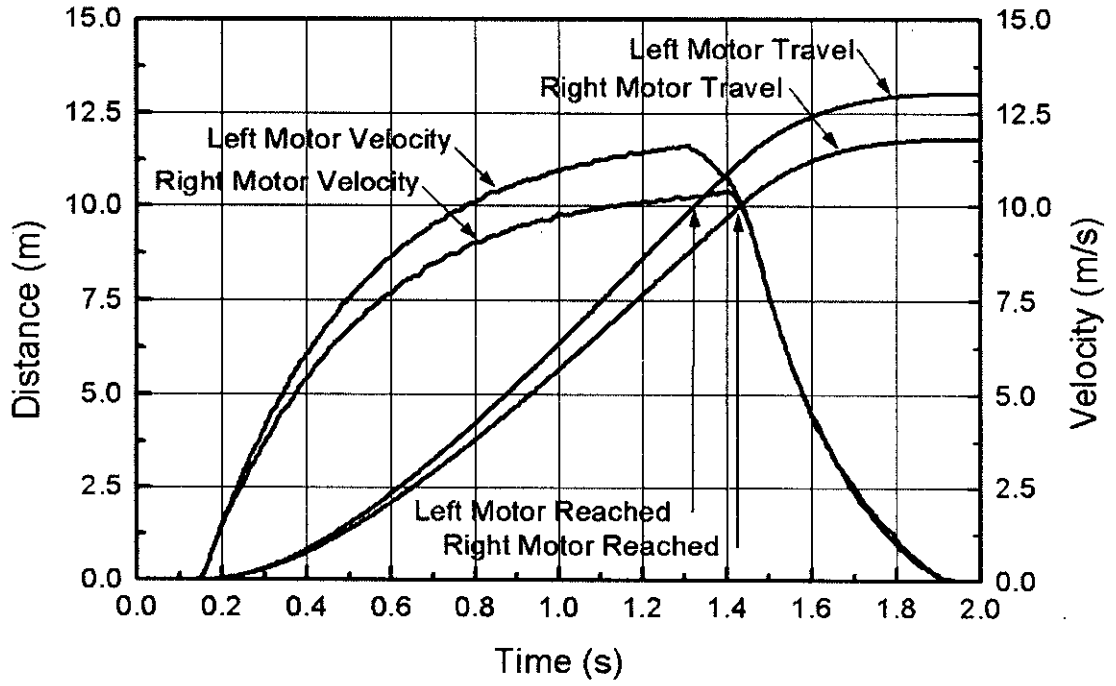


Fig. 5.4. Motor traverse and the corresponding velocity (unloaded motors with 100% duty cycle).

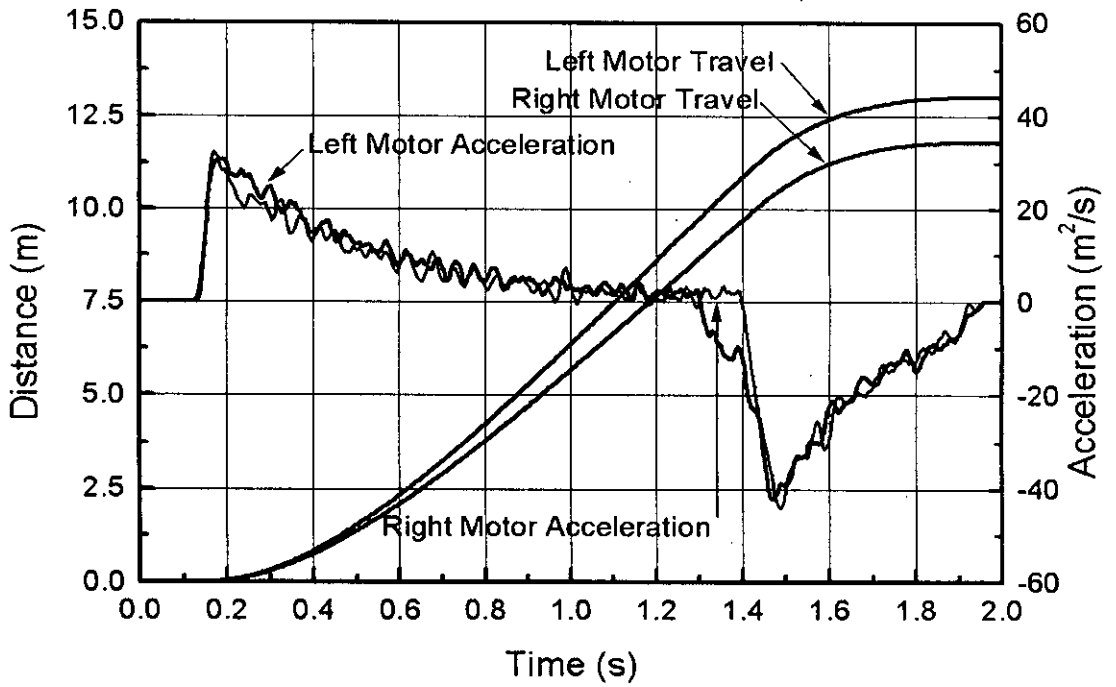


Fig. 5.5. Motor traverse and the corresponding acceleration (unloaded motors with 100% duty cycle).

In Fig. 5.5, the accelerations of the motors are presented. It is clearly seen that there is very high acceleration at the beginning of the journey although it resulted in very low initial velocity. The high initial acceleration is observed because of the initiation of motion from rest. The motor acceleration demands high motor current and it is clearly observed in the present study, as shown in Fig. 5.6. Motor current pattern closely follows the motor acceleration pattern, at the beginning of the journey the left motor acceleration and the currents are high but at the end of the journey the right motor acceleration and the associated current flows are high. However, after reaching the set distance of 10 m, the motor currents are zeroed and dynamic braking is applied. Initially, generated back emf created forces opposite to the rotation direction and the deceleration rate is high. Once the kick of eddy current is reduces, the braking mechanism is less effective. Dynamic braking provides a path to the conduct current generated by the back emf and results in modest braking which is evident in the final stages of the motion.

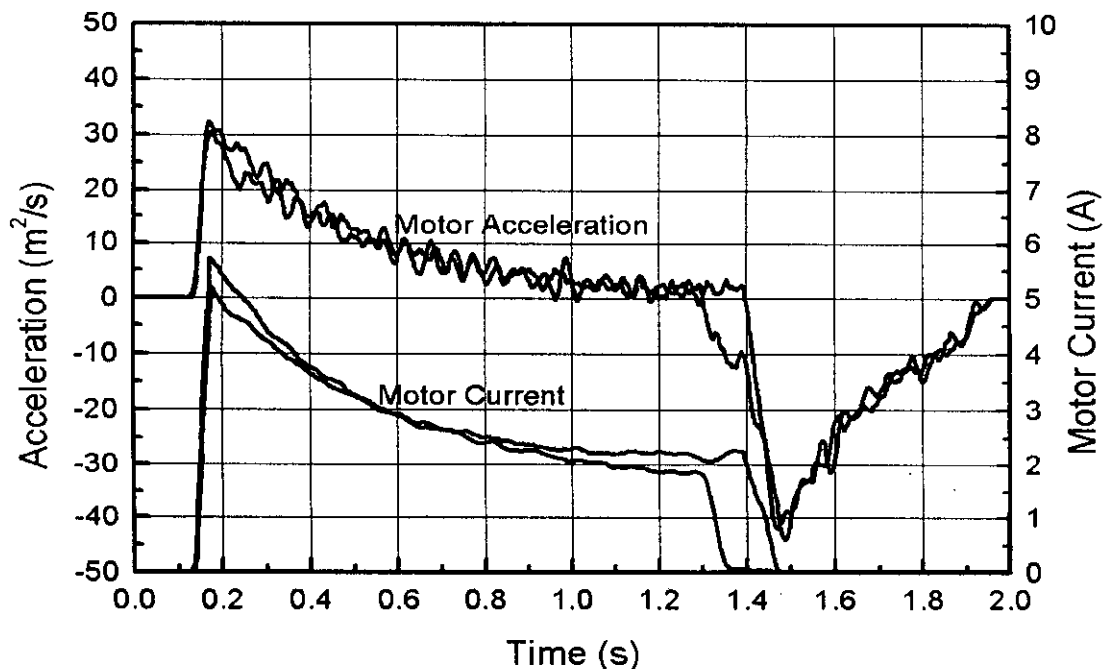


Fig. 5.6. Motor acceleration and the corresponding current (unloaded motors with 100% duty cycle).

In Figs. 5.1-5.6, various parameters are shown for the unloaded robot motors. The unloaded condition is achieved by lifting the robot, i.e. wheels not touching floor. Motors run and stop fast, however motor current is not insignificant because of friction of various components although these are not providing traction. Shown in Figs. 5.7-5.11 are the various parameters obtained for the motors when the robot is running with a total self weight of 13.5 Kg. It is observed that the robot could not attain uniform velocity even after traversing set distance of 10 m. Both the values of motor speed and acceleration are lower but the motor currents are significantly higher. At the end of the travel, robot is physically stopped which is clearly indicated in Figs. 5.10 and 5.11, where velocity is suddenly dropped and deceleration is with a very high value.

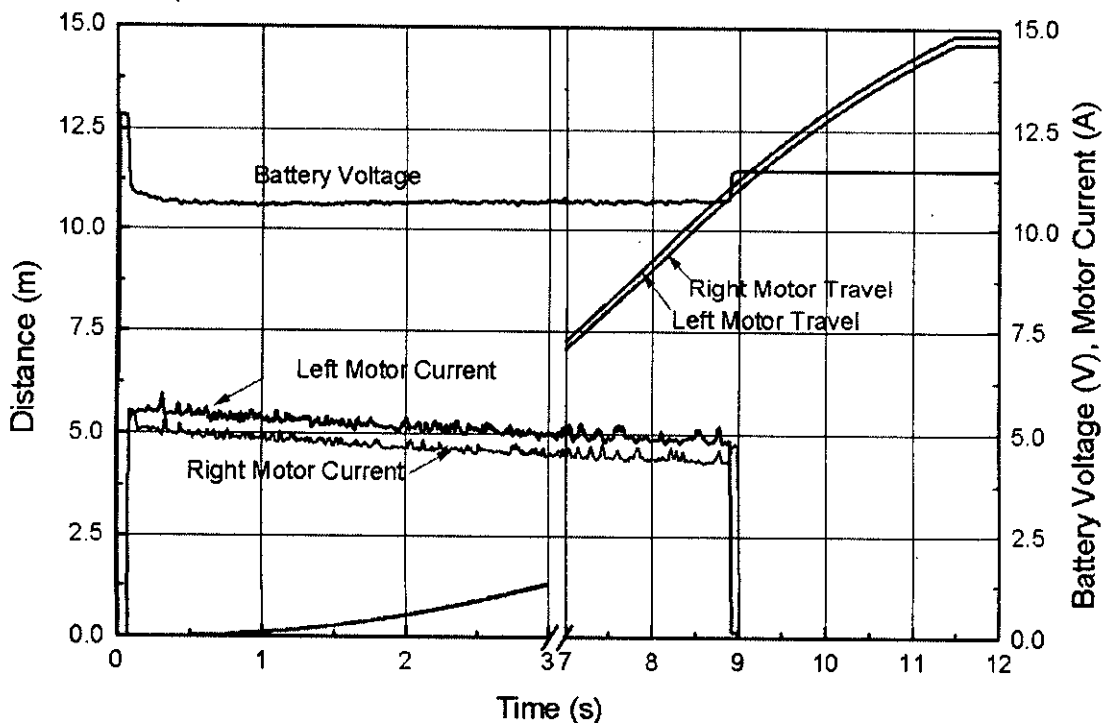


Fig. 5.7. Motor traverse and the corresponding motor currents and battery voltage (wheel load 13.5 Kg and motor PWM with 100% duty cycle).

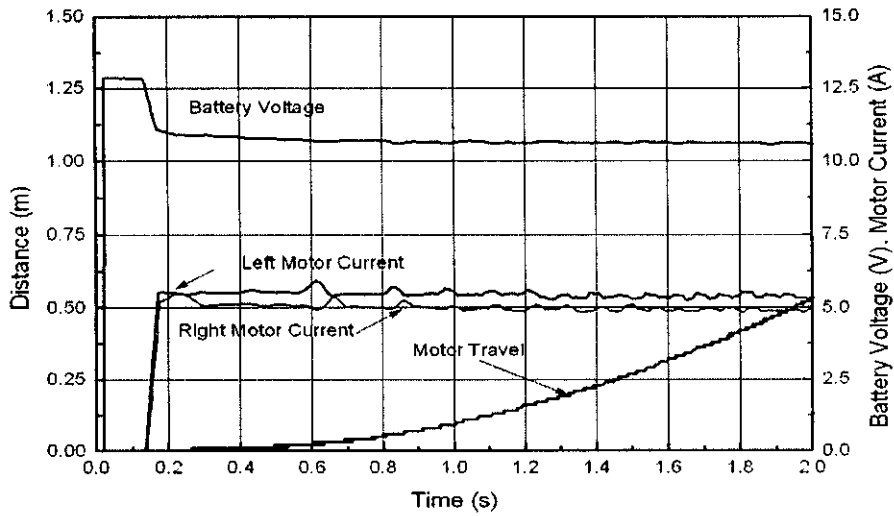


Fig. 5.8. Motor traverse and the motor currents and battery voltage at the early stage of the motion (wheel load 13.5 Kg and motor PWM with 100% duty cycle).

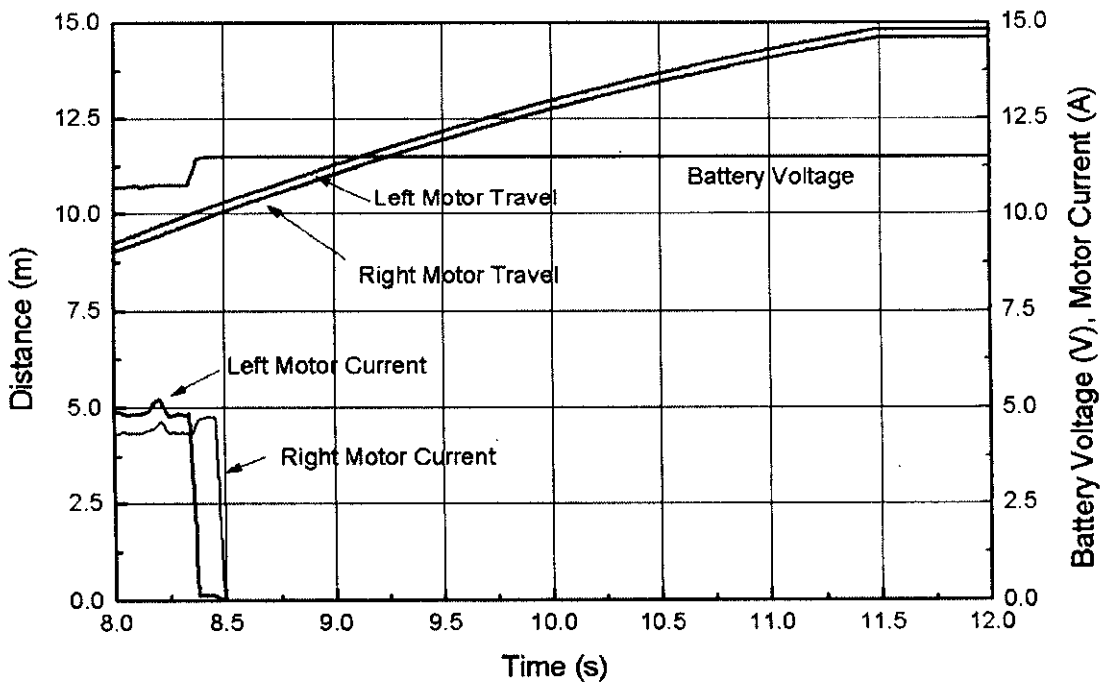


Fig. 5.9. Motor traverse and the motor currents and battery voltage at the final stage of the motion (wheel load 13.5 Kg and motor PWM with 100% duty cycle).



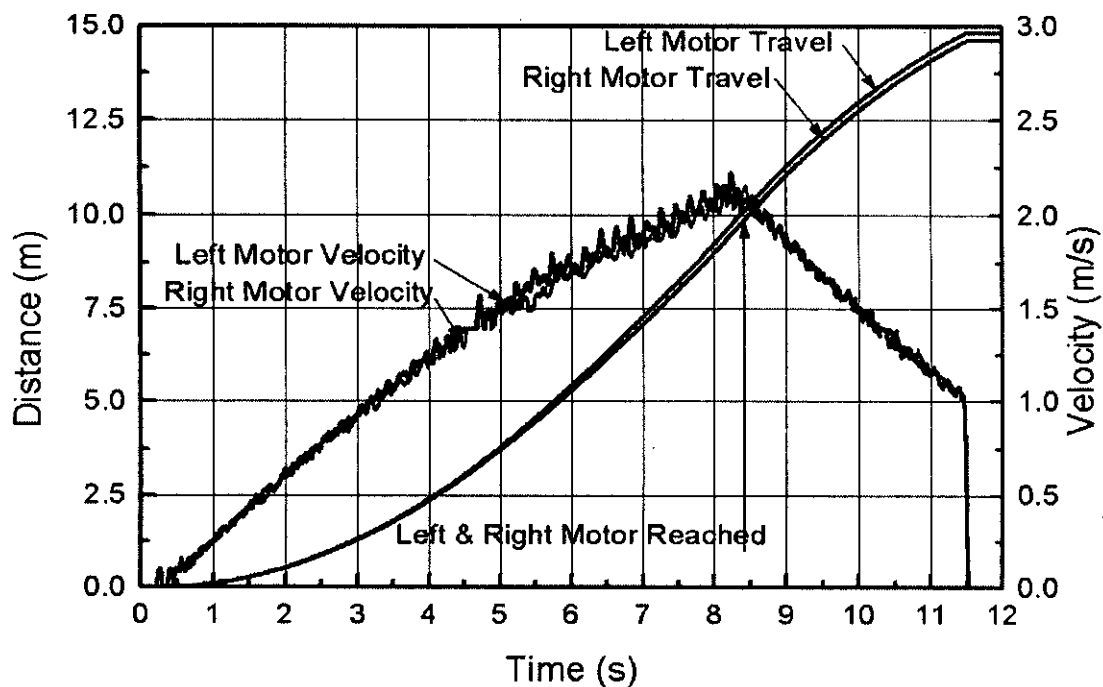


Fig. 5.10. Motor traverse and the corresponding velocity (wheel load 13.5 Kg and motor PWM with 100% duty cycle).

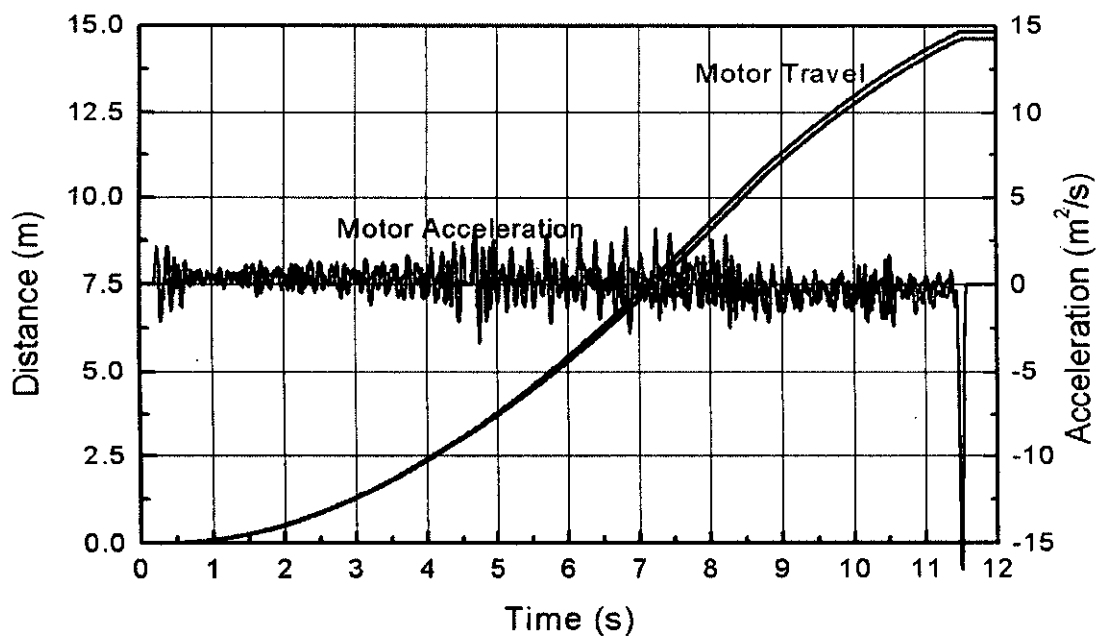


Fig. 5.11. Motor traverse and the corresponding acceleration (wheel load 13.5 Kg and motor PWM with 100% duty cycle).

The effects of further loading on the robot dynamics is further investigated by adding 6.5 Kg of load on the robot, and therefore robot wheel load become 20.0 Kg. The motion parameters, battery voltage and motor currents are shown in Figs. 5.12-16. Significant slowing down of the robot is observed with increase in motor current. The motors consume more current to start, acceleration is slow, peak velocity is significantly lower. Robot could not attain uniform velocity even after traveling 15 m, and the robot is physically stopped. Physical stop is clearly visible in Figs. 5.15 and 5.16. Motor currents are significantly higher with associated higher battery voltage drop which recovered significantly after there is no motor current demand.

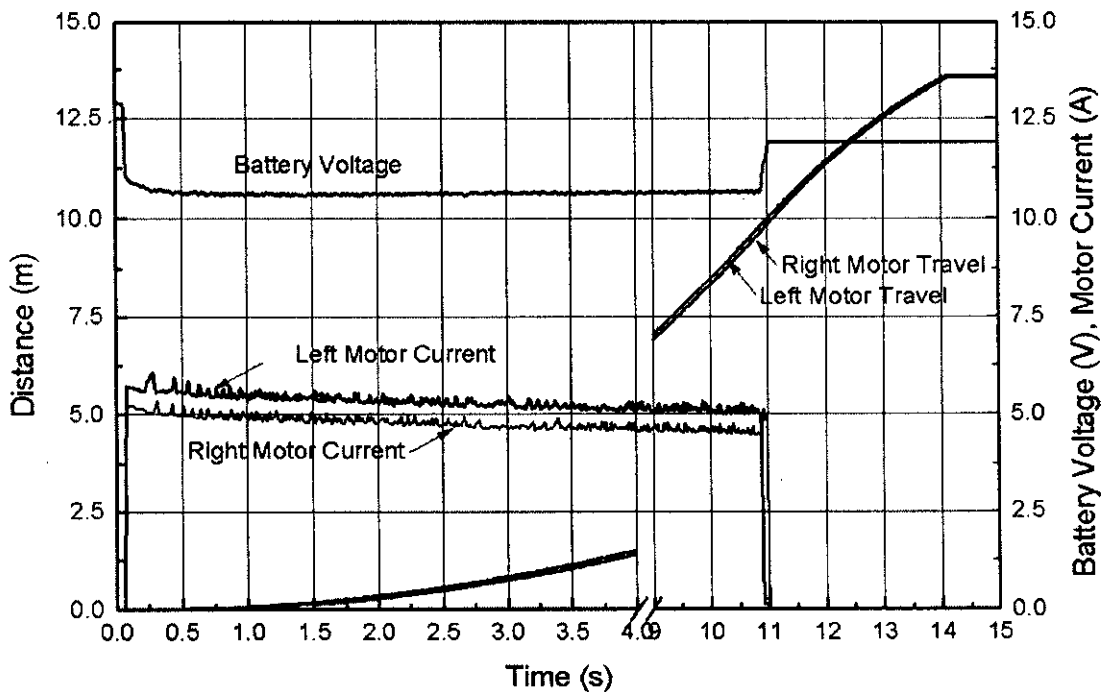


Fig. 5.12. Motor traverse and the corresponding motor currents and battery voltage (wheel load 20.0 Kg and motor PWM with 100% duty cycle).

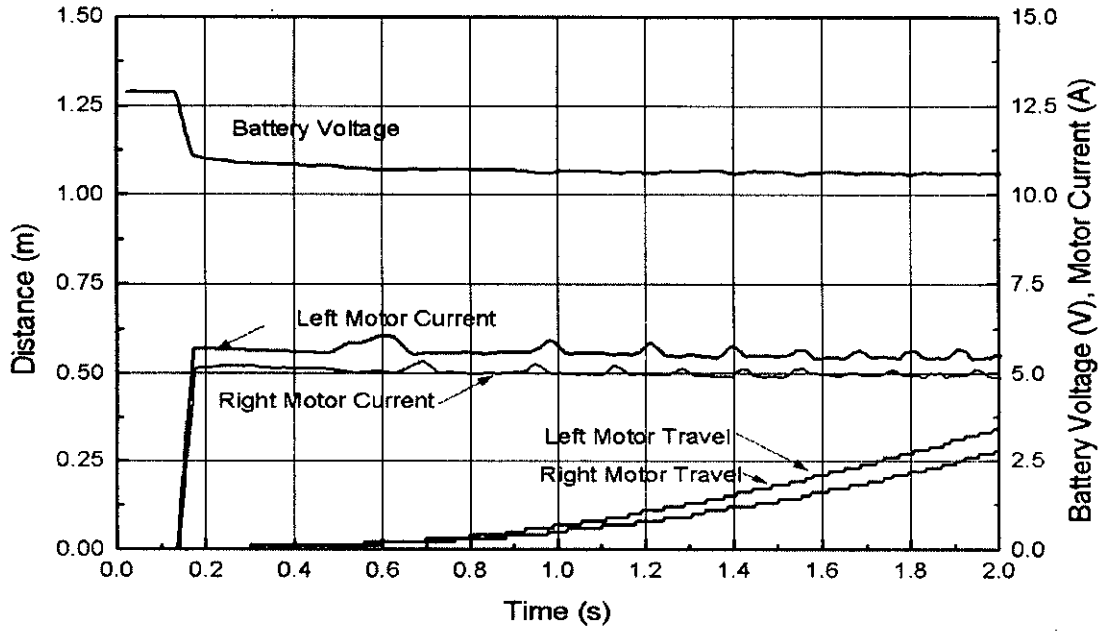


Fig. 5.13. Motor traverse and the motor currents and battery voltage at the early stage of the motion (wheel load 20.0 Kg and motor PWM with 100% duty cycle).

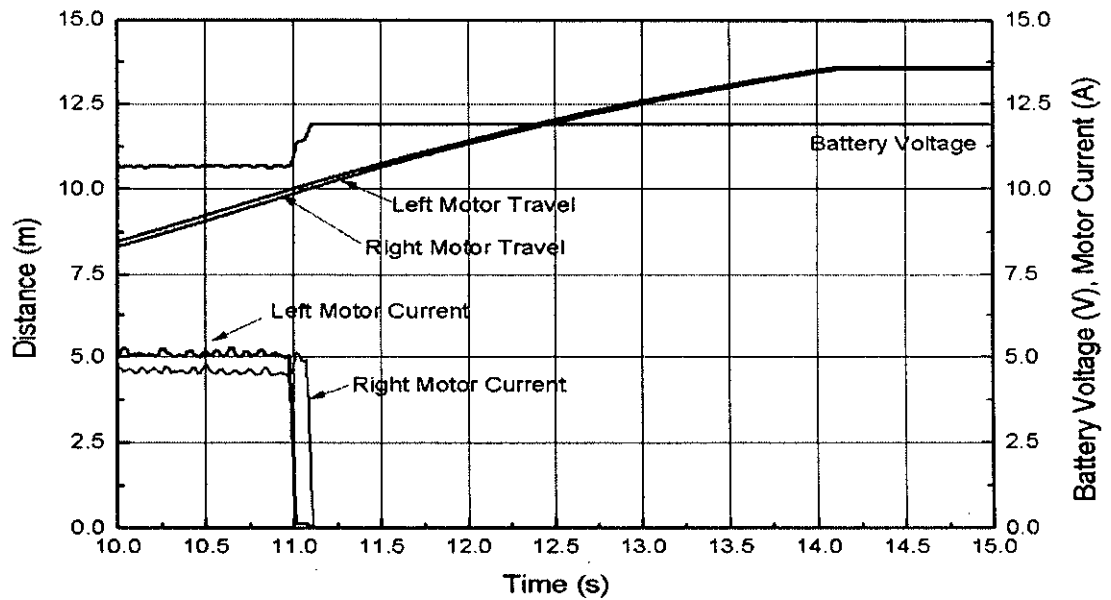


Fig. 5.14. Motor traverse and the motor currents and battery voltage at the final stage of the motion (wheel load 20.0 Kg and motor PWM with 100% duty cycle).

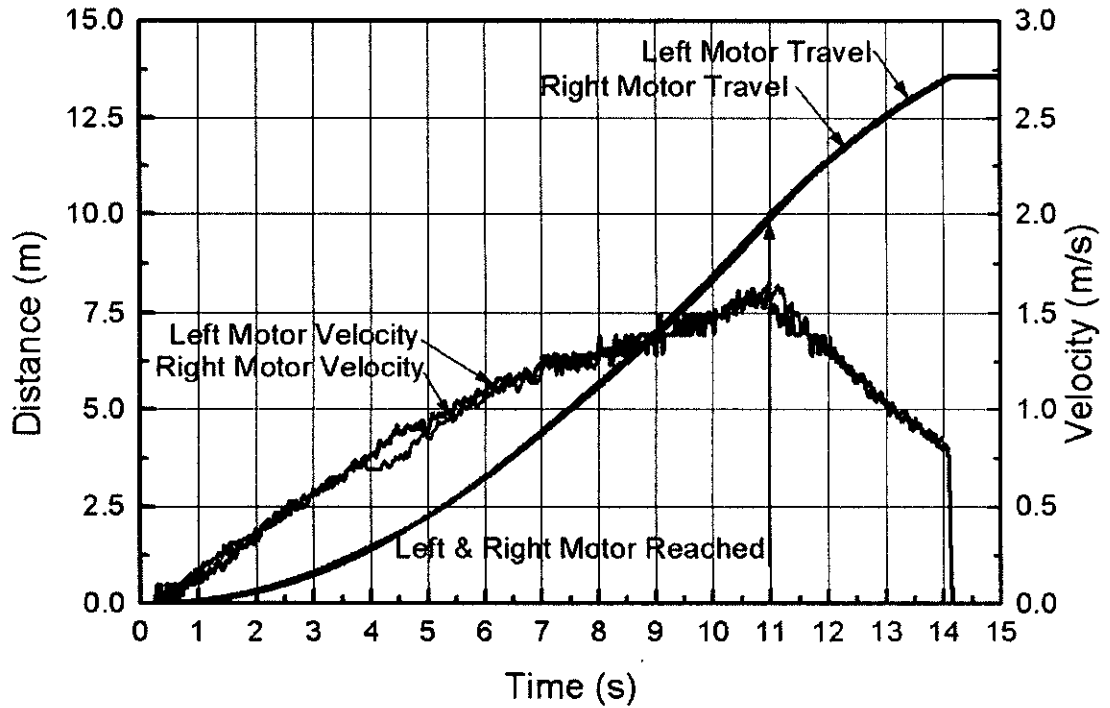


Fig. 5.15. Motor traverse and the corresponding velocity (wheel load 20.0 Kg and motor PWM with 100% duty cycle).

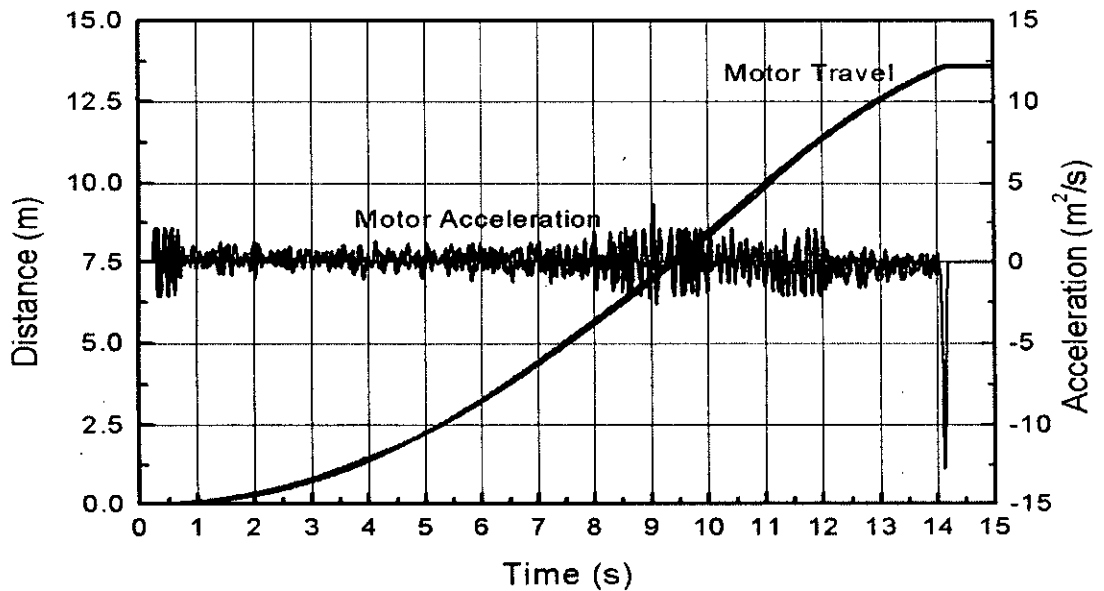


Fig. 5.16. Motor traverse and the corresponding acceleration (wheel load 20.0 Kg and motor PWM with 100% duty cycle).

In the experiments shown in Figs. 5.1-5.16, motors are powered by PWM with 100% duty cycle. In an ideal case, the robot should provide similar motion characteristics and therefore straight motion. But in the present experiments, the left motor runs faster to result in slightly curved motion. Hence, to reduce power of the left motor, it is run by PWM at 90% and 85% duty cycle while keeping 100% duty cycle in the right motor. Corresponding traversed distance and velocity are shown in Figs. 5.17 and 5.18 respectively. Very little difference in motion parameters are observed in case of duty cycle of 90%, and the difference between motors diminishes further in case of left motor powered at 85% duty cycle while keeping 100% duty cycle at the right motor. Fig. 5.18 shows nearly identical parameters for both the motors and therefore can be considered as the optimum duty cycle for straight motion. This optimum duty cycle is experimentally verified for loaded conditions as shown in Figs. 5.19-5.33.

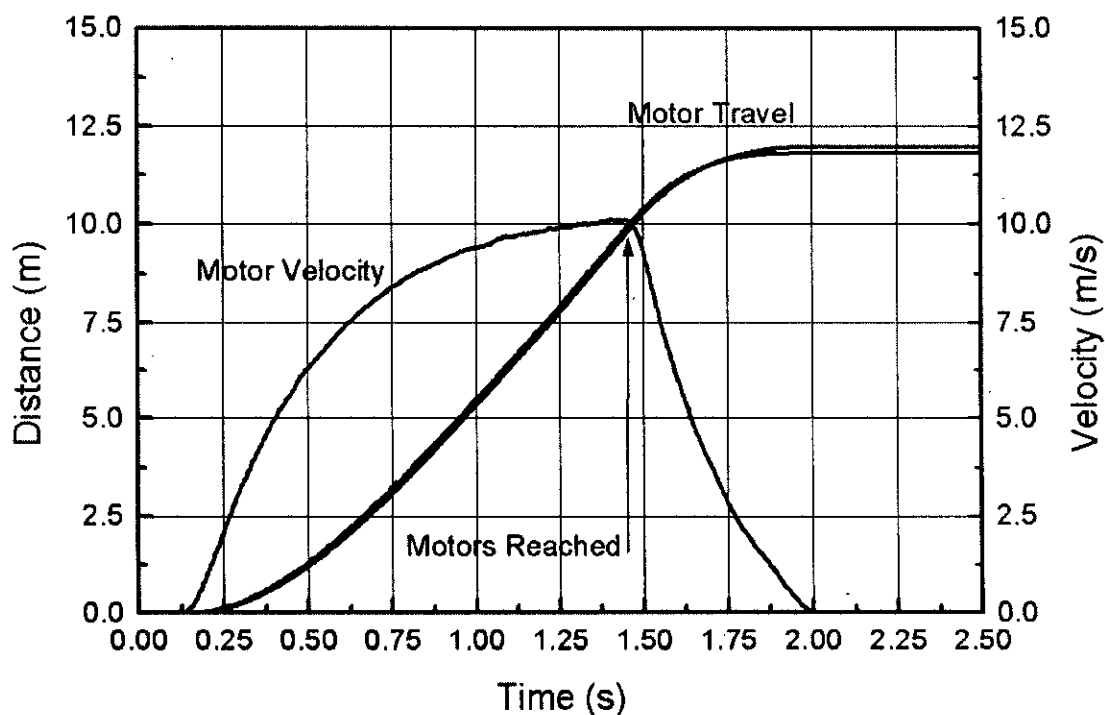


Fig. 5.17. Motor traverse and the corresponding velocity (unloaded motors with 100% duty cycle at right motor and 90% duty cycle at the left).

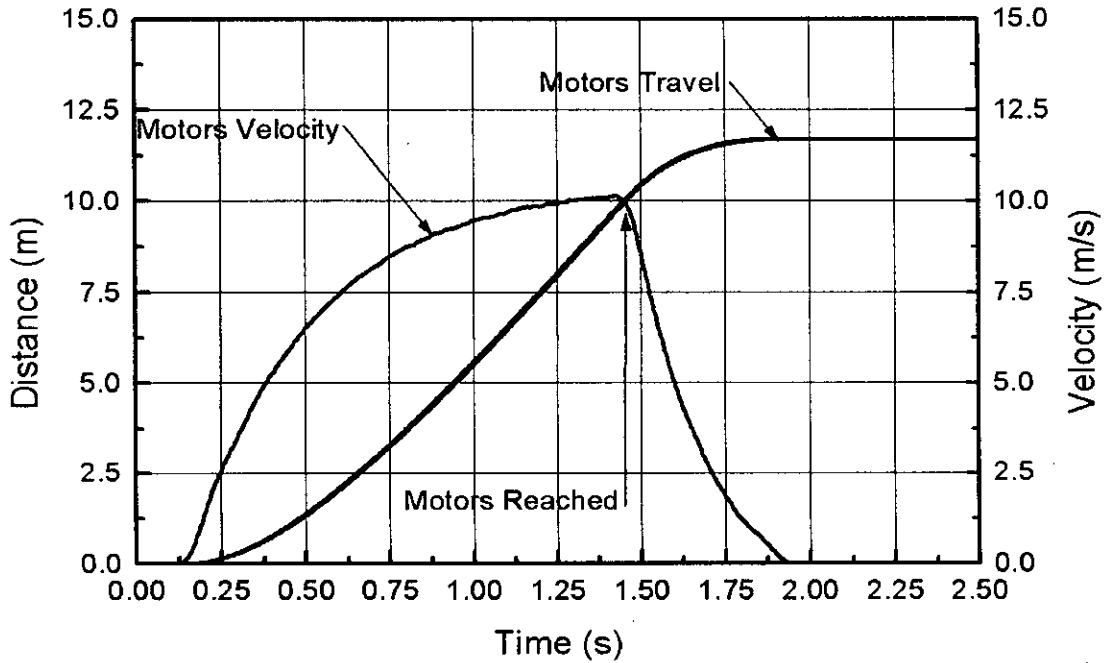


Fig. 5.18. Motor traverse and the corresponding velocity (unloaded motors with 100% duty cycle at right motor and 85% duty cycle at the left).

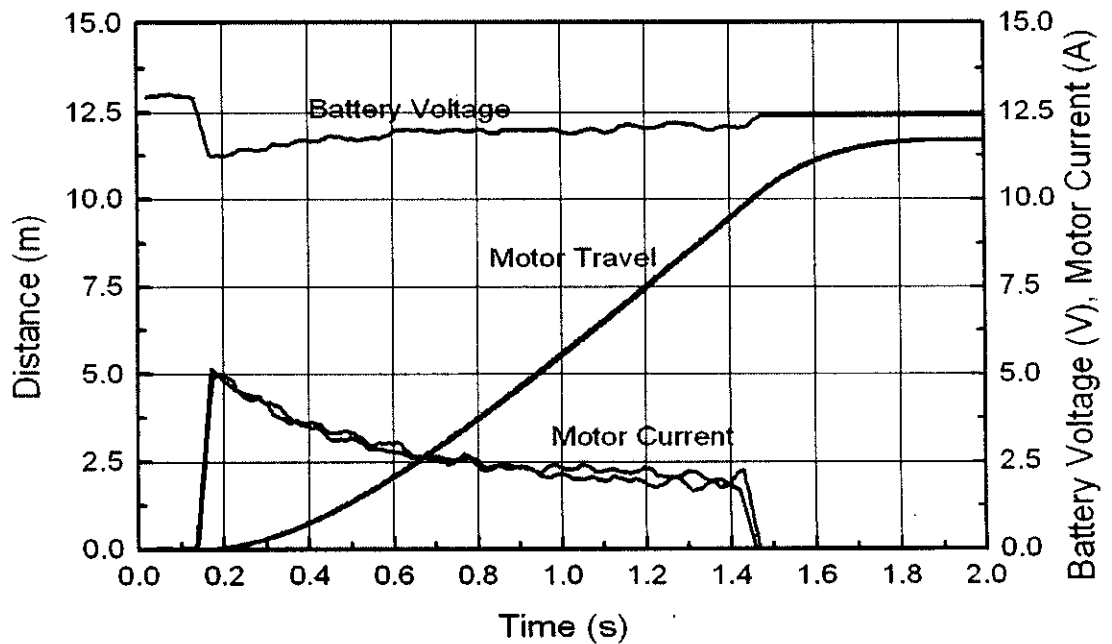


Fig. 5.19. Motor traverse and the corresponding motor currents and battery voltage (unloaded motors with 100% duty cycle at right motor, 85% at left motor).

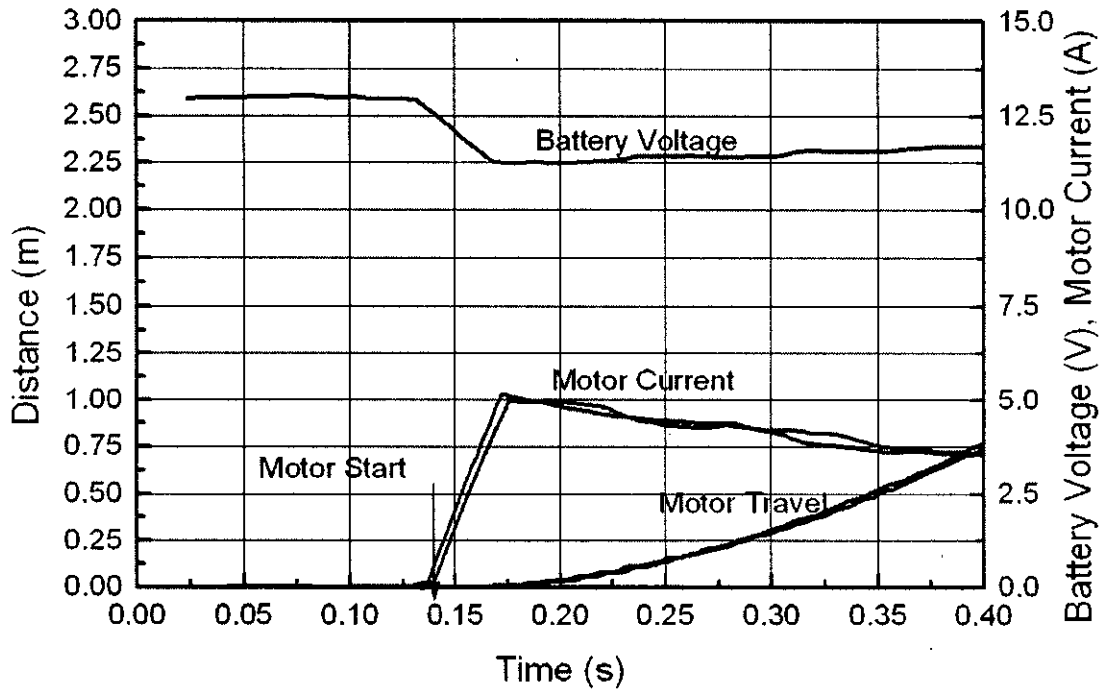


Fig. 5.20. Motor traverse and motor currents and battery voltage at the early stage of motion (unloaded motors, 100% duty cycle at right and 85% duty cycle at the left).

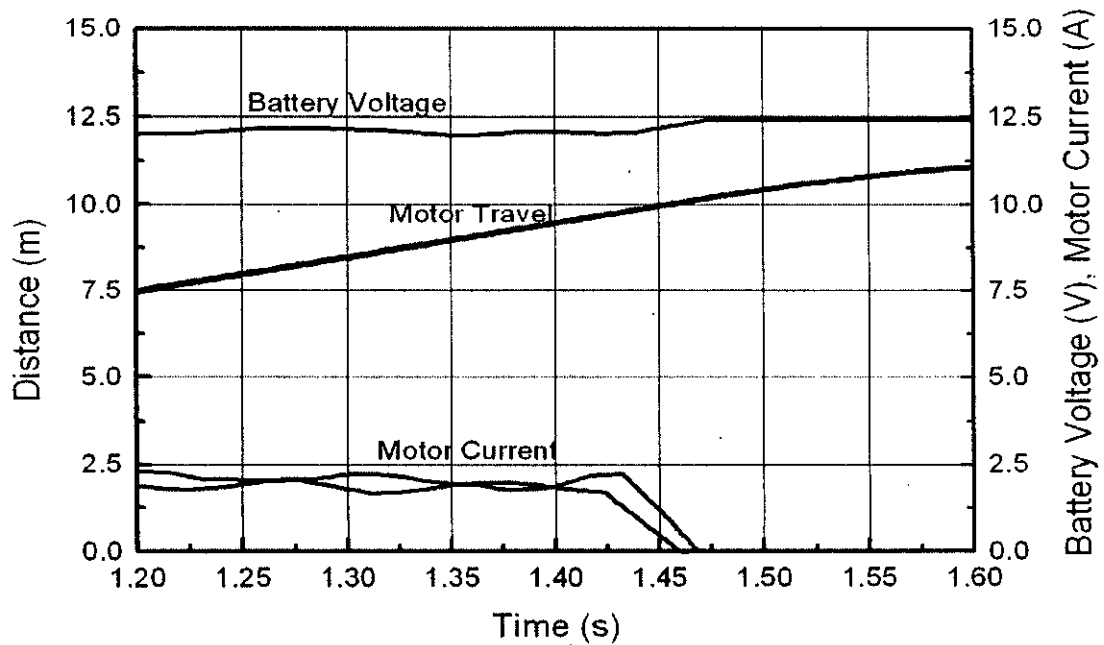


Fig. 5.21. Motor traverse and motor currents and battery voltage at the final stage of motion (unloaded motors, 100% duty cycle at right and 85% duty cycle at the left).

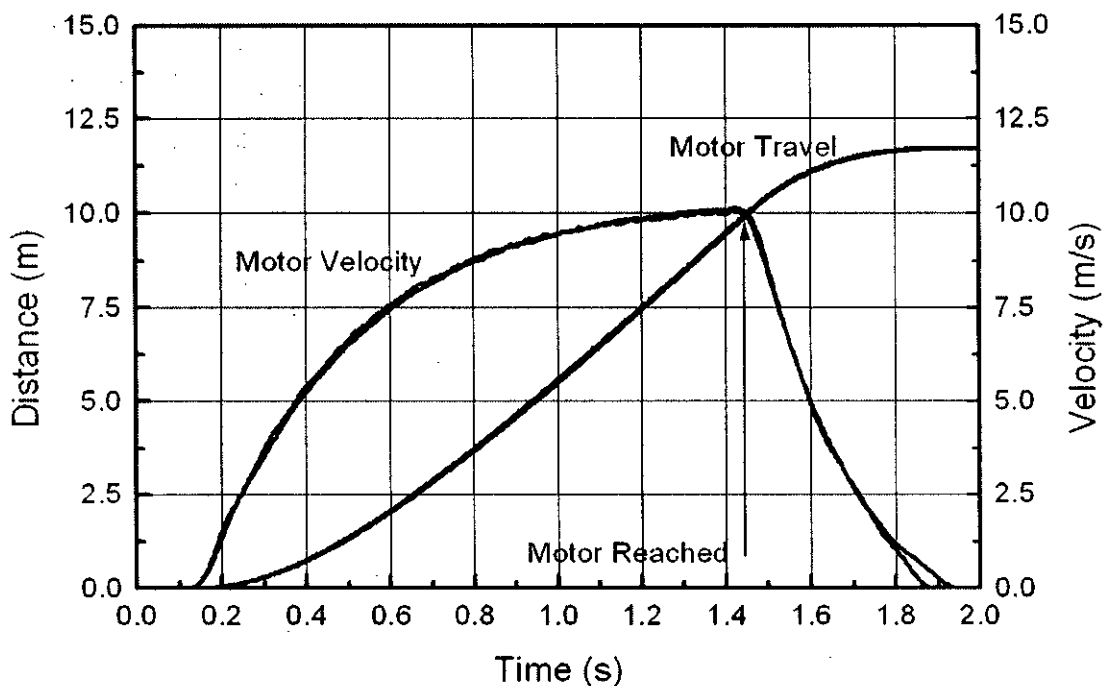


Fig. 5.22. Motor traverse and the corresponding velocity (unloaded motors with 100% duty cycle at right motor and 85% duty cycle at the left).

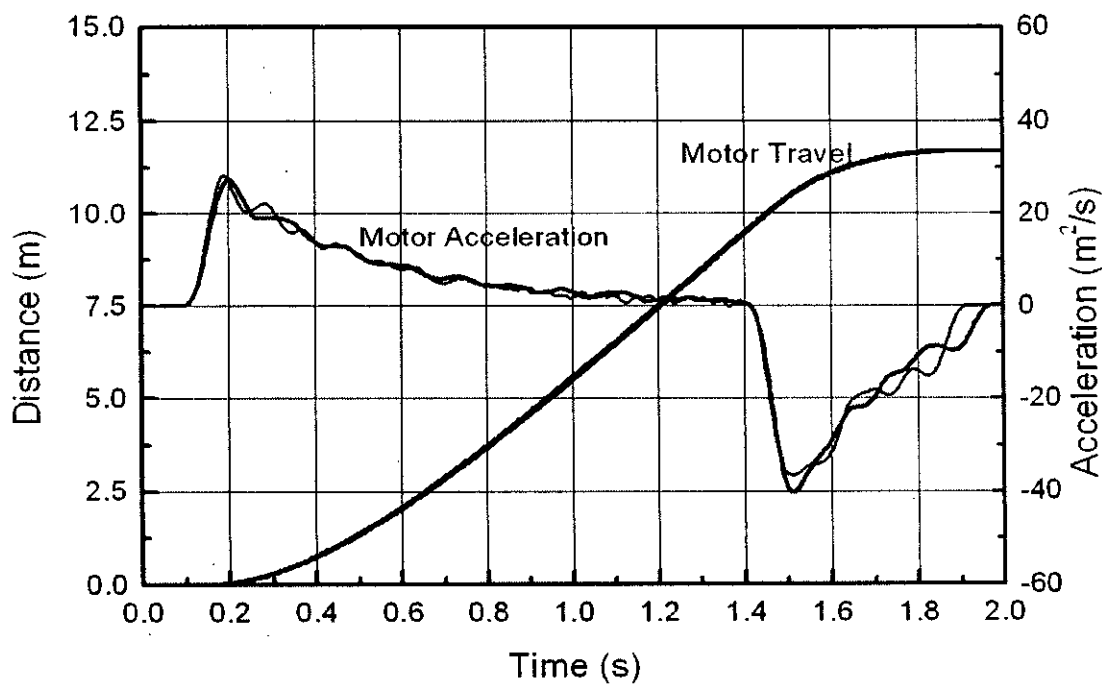


Fig. 5.23. Motor traverse and the corresponding acceleration (unloaded motors with 100% duty cycle at right motor and 85% duty cycle at the left).



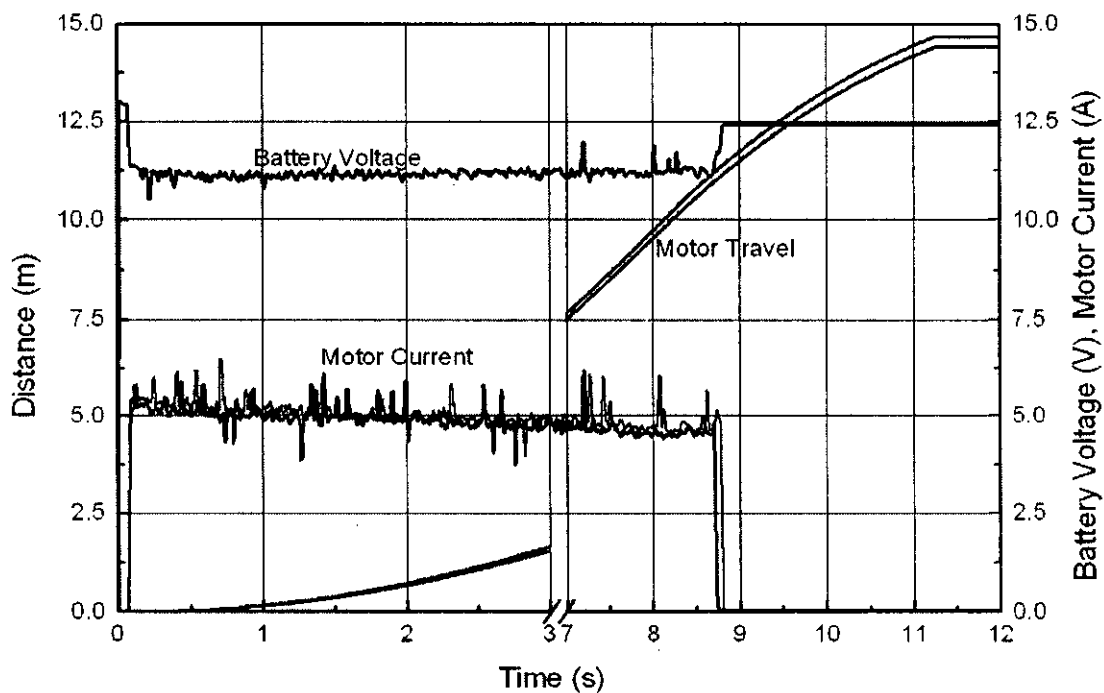


Fig. 5.24. Motor traverse and motor currents and battery voltage (wheel load 13.5 Kg with 100% duty cycle at right motor and 85% duty cycle at the left).

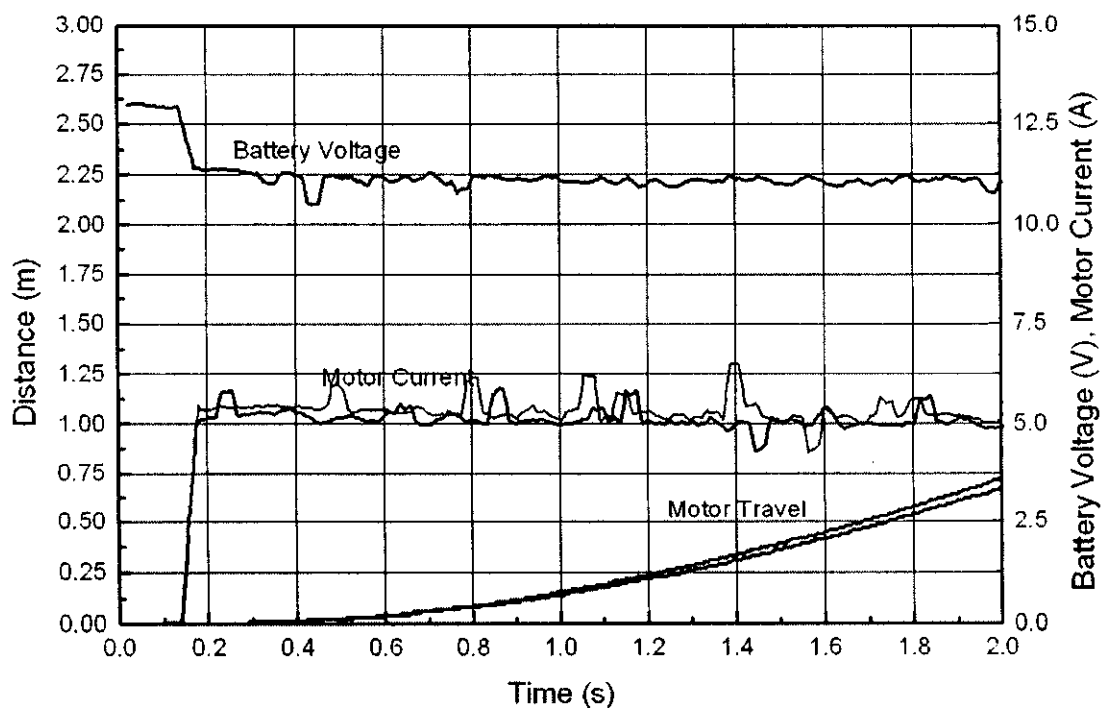


Fig. 5.25. Motor traverse, currents and battery voltage at the early stage of motion (wheel load 13.5 Kg, 100% duty cycle at right and 85% duty cycle at the left).

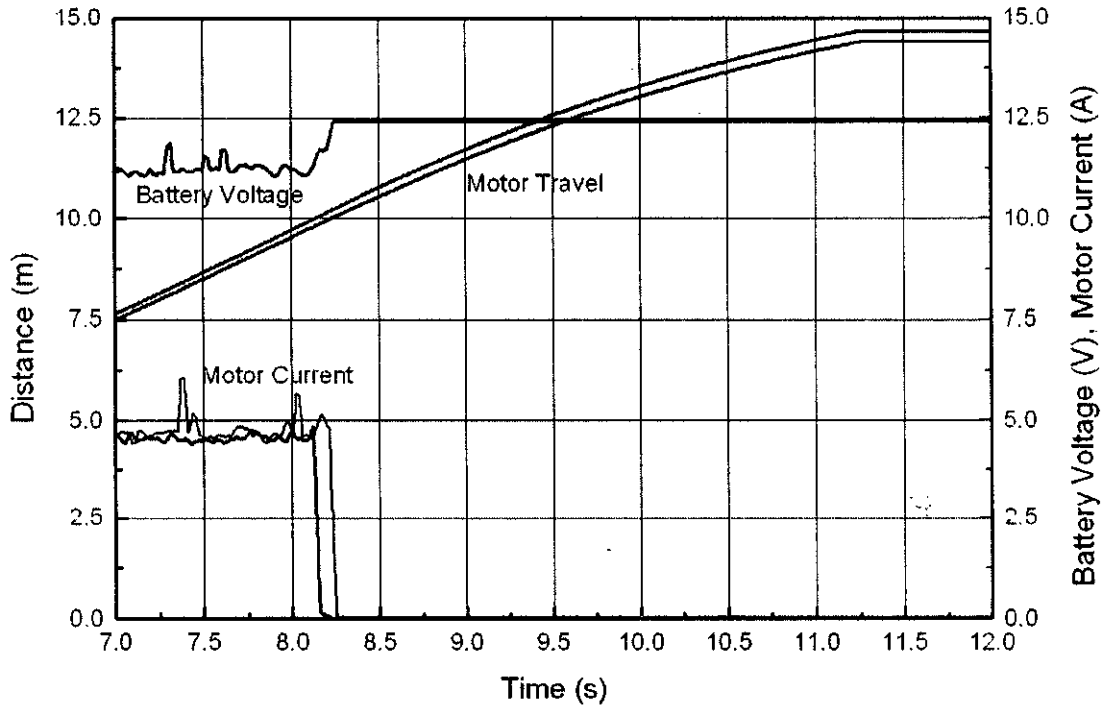


Fig. 5.26. Motor traverse and currents and battery voltage at the final stage of motion (wheel load 13.5 Kg, 100% duty cycle at right motor and 85% duty cycle at the left).

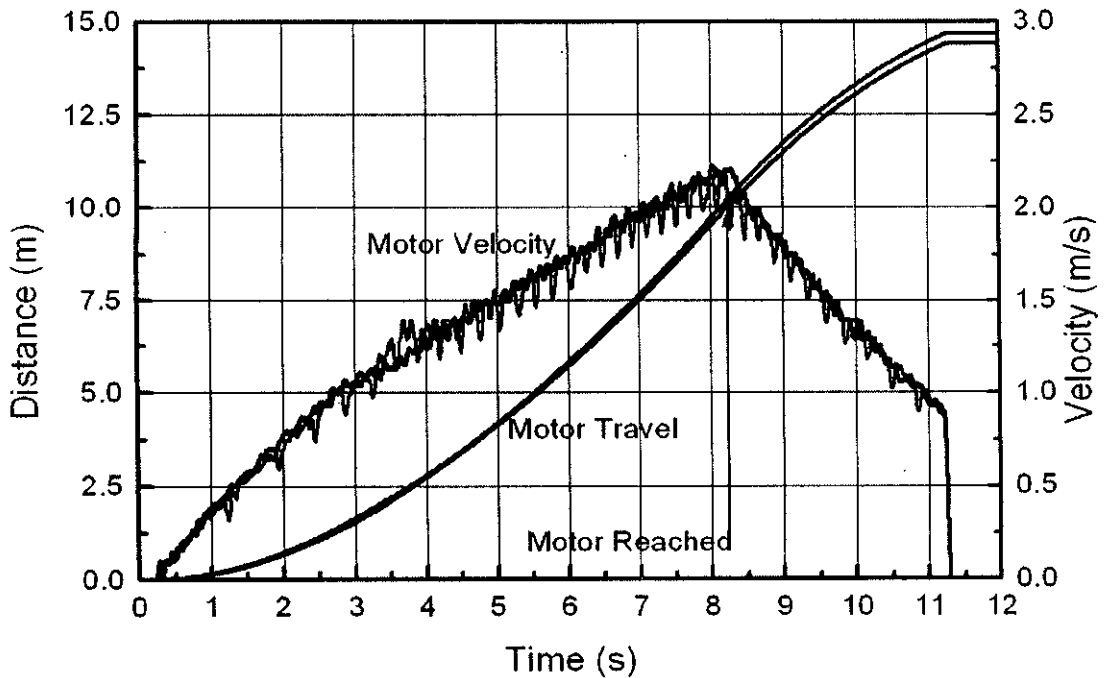


Fig. 5.27. Motor traverse and the corresponding velocity (wheel load 13.5 Kg with 100% duty cycle at right motor and 85% duty cycle at the left).

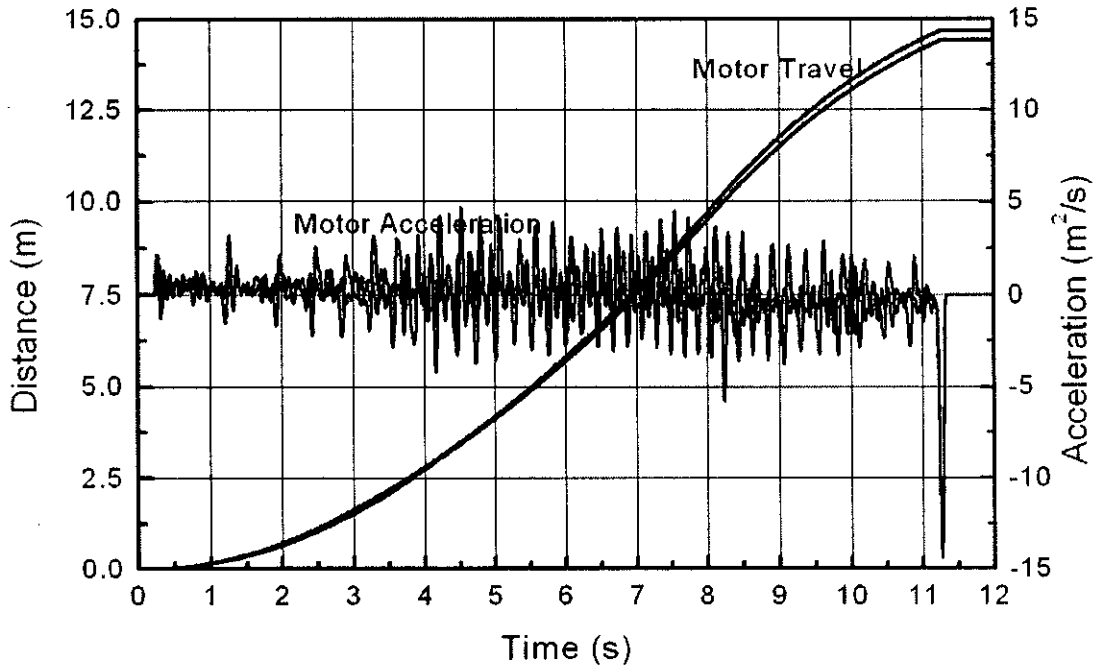


Fig. 5.28. Motor traverse and the corresponding acceleration (wheel load 13.5 Kg with 100% duty cycle at right motor and 85% duty cycle at the left).

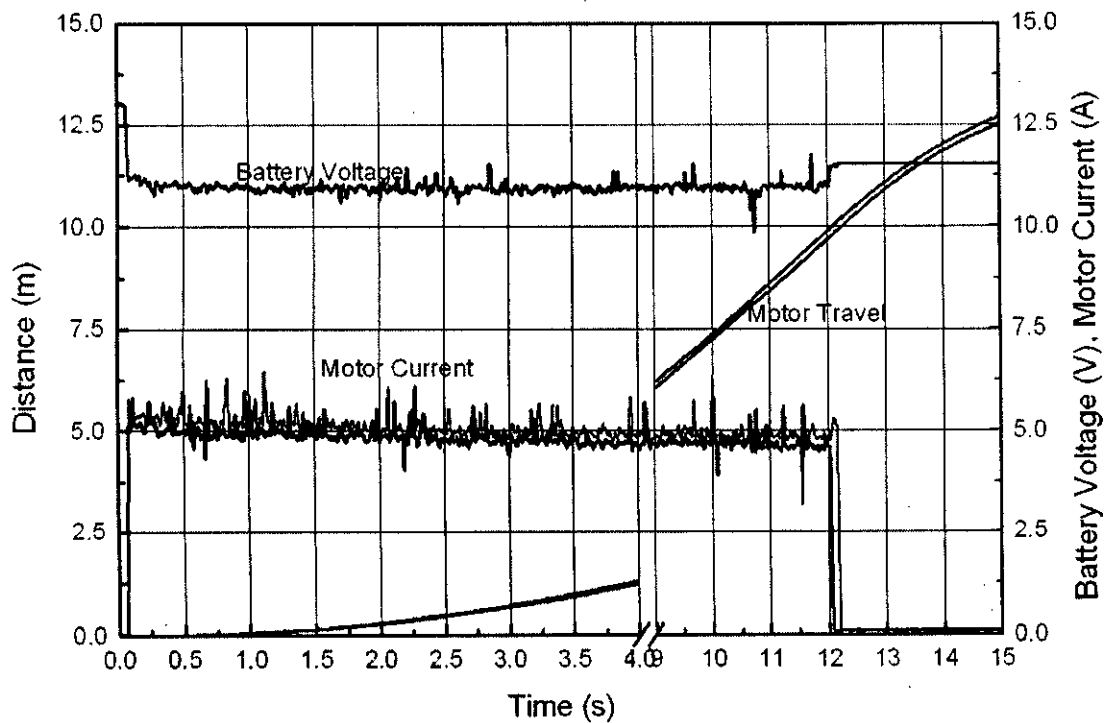


Fig. 5.29. Motor traverse and motor currents and battery voltage (wheel load 20.0 Kg with 100% duty cycle at right motor and 85% duty cycle at the left).

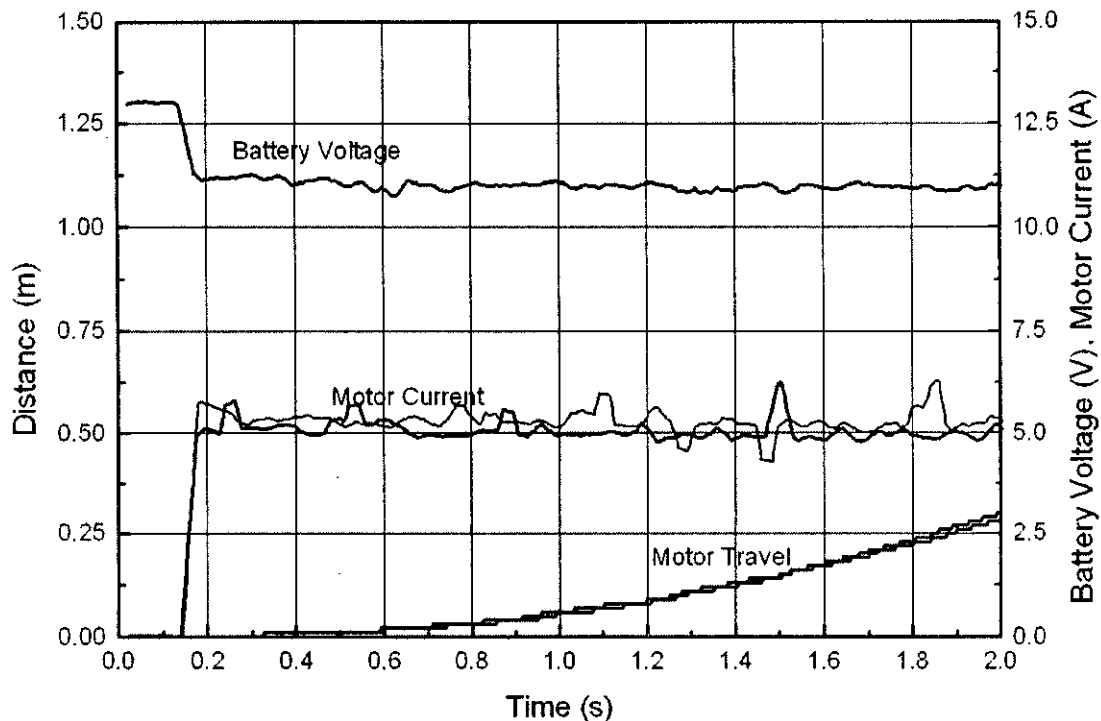


Fig. 5.30. Motor traverse and currents and battery voltage at early stage of motion (wheel load 20.0 Kg, 100% duty cycle at right and 85% duty cycle at the left).

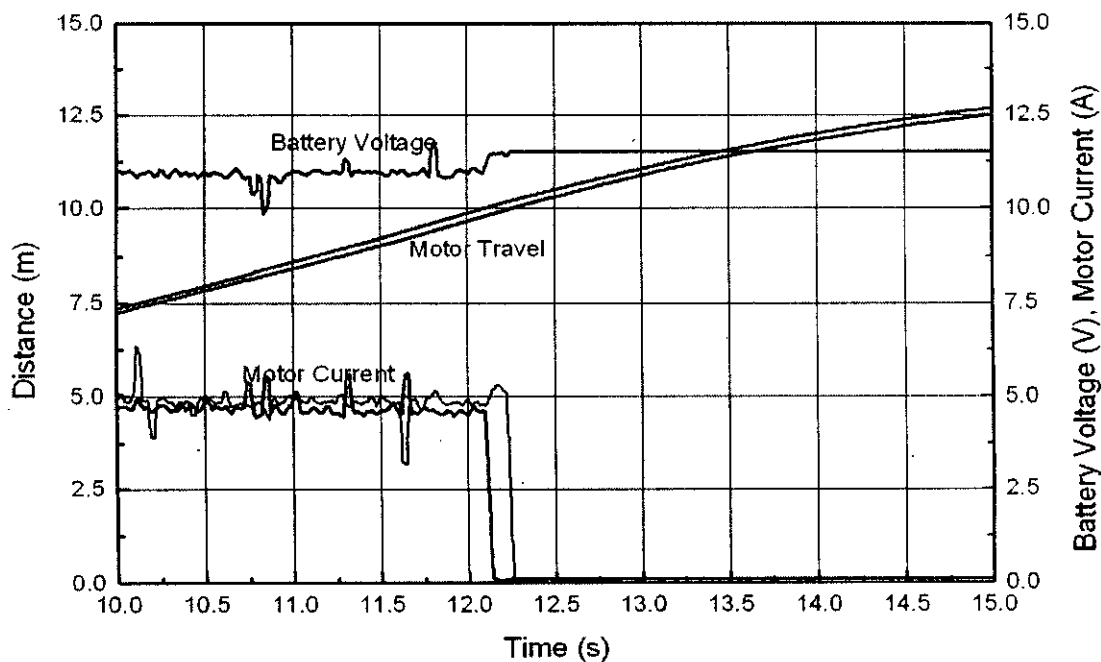


Fig. 5.31. Motor traverse and currents and battery voltage at the final stage of the motion (wheel load 20.0 Kg, 100% duty cycle at right and 85% duty cycle at left).

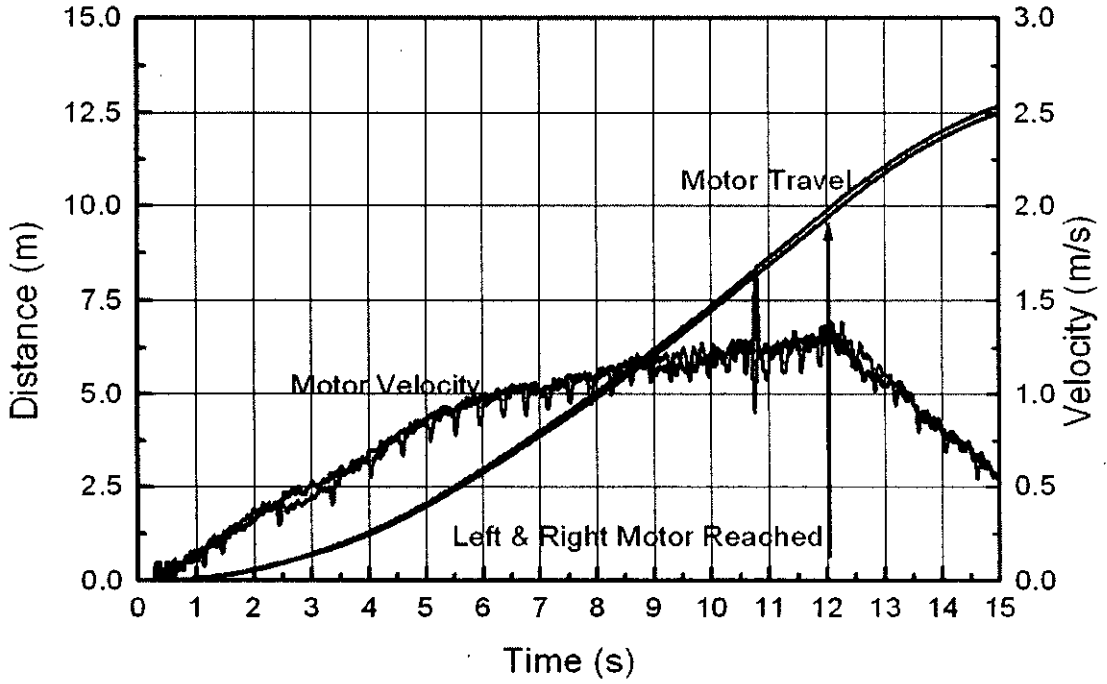


Fig. 5.32. Motor traverse and the corresponding velocity (wheel load 20.0 Kg with 100% duty cycle at right motor and 85% duty cycle at the left).

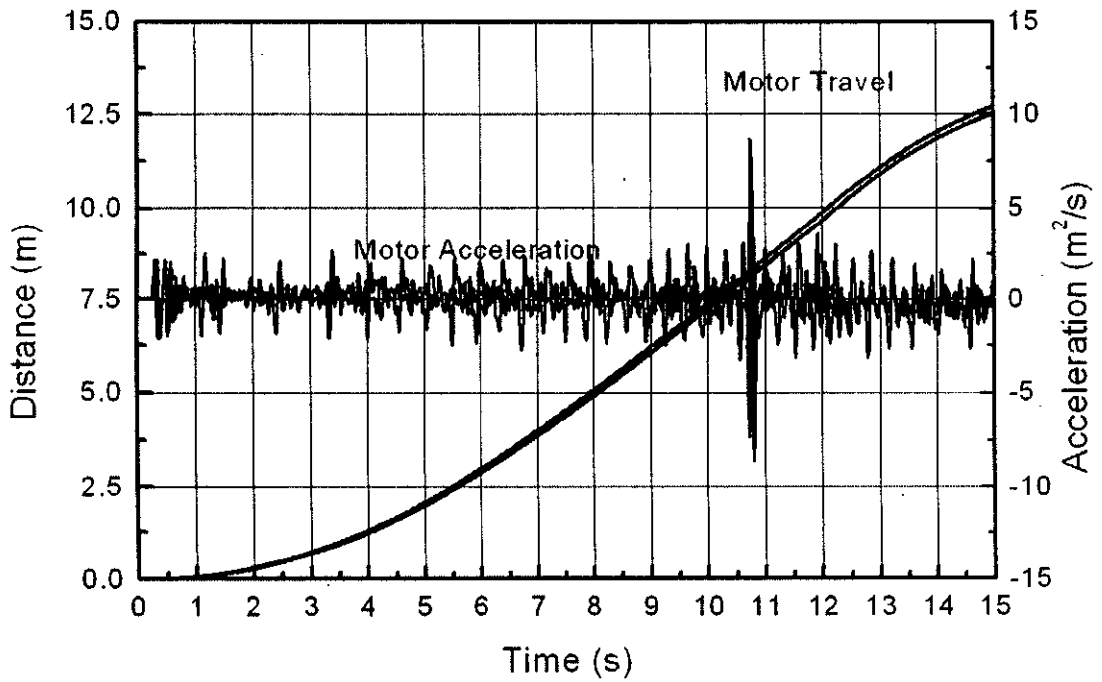


Fig. 5.33. Motor traverse and the corresponding acceleration (wheel load 20.0 Kg with 100% duty cycle at right motor and 85% duty cycle at the left).

Shown in Figs. 5.34-5.36 are the effects of loading on the robot motion. In these figures, data for left motors are plotted as at 100% duty cycle at right motor and 85% duty cycle at left motor make the motor characteristics very close. It is seen in Fig. 5.34, time taken to traverse a distance of 10 m is small in case of unloaded motor. However, significant time (approx 8 sec in case of 13.5 Kg wheel load and 12 sec in case of 20.0 Kg wheel load) is required in case of loaded robot, required time is 1.5 times higher in case of 1.5 times load. It is clearly seen in Fig. 5.35 that the heavier robot takes more time to start its motion. Shown in Fig. 5.36 are the effect of loading on robot velocity. The effect of loading to reduce the robot speed is clearly seen in the figure. Effect of load on the motor current is also demonstrated in Fig. 5.37. It is clearly seen that motor currents increase with wheel loading and the motor currents decreased with increase in time and motor speed. In all these cases, motor currents stop after these traverse 10 m distance.

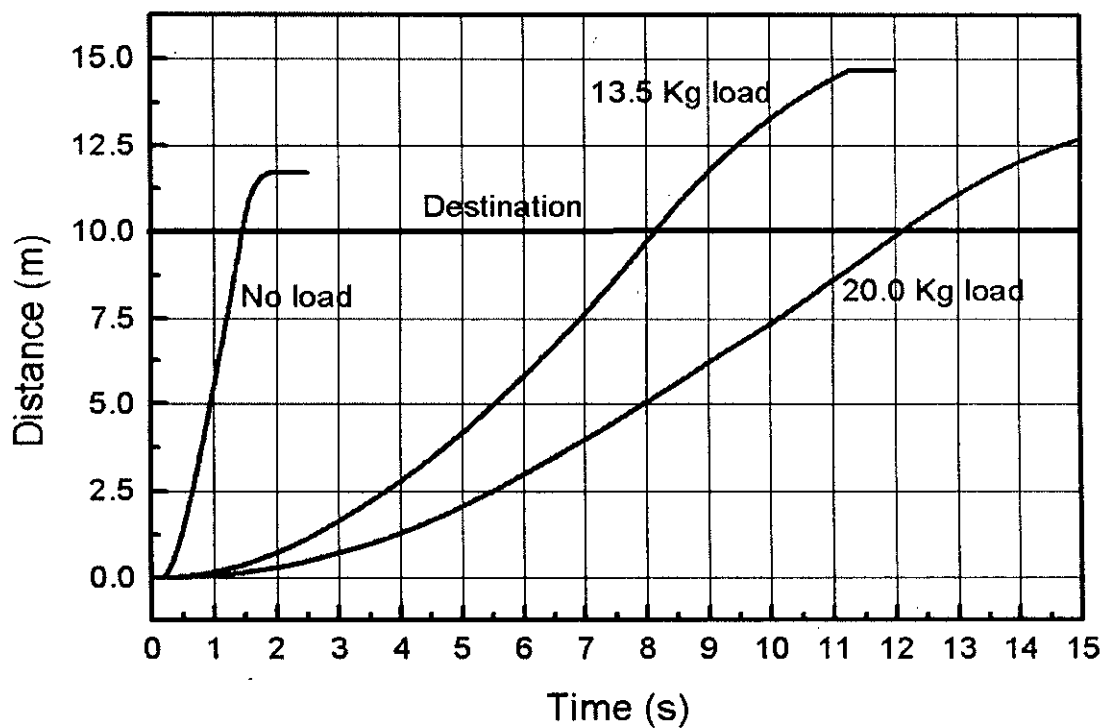


Fig. 5.34. Effect of load on motor traverse (100% duty cycle at right motor and 85% duty cycle at the left).

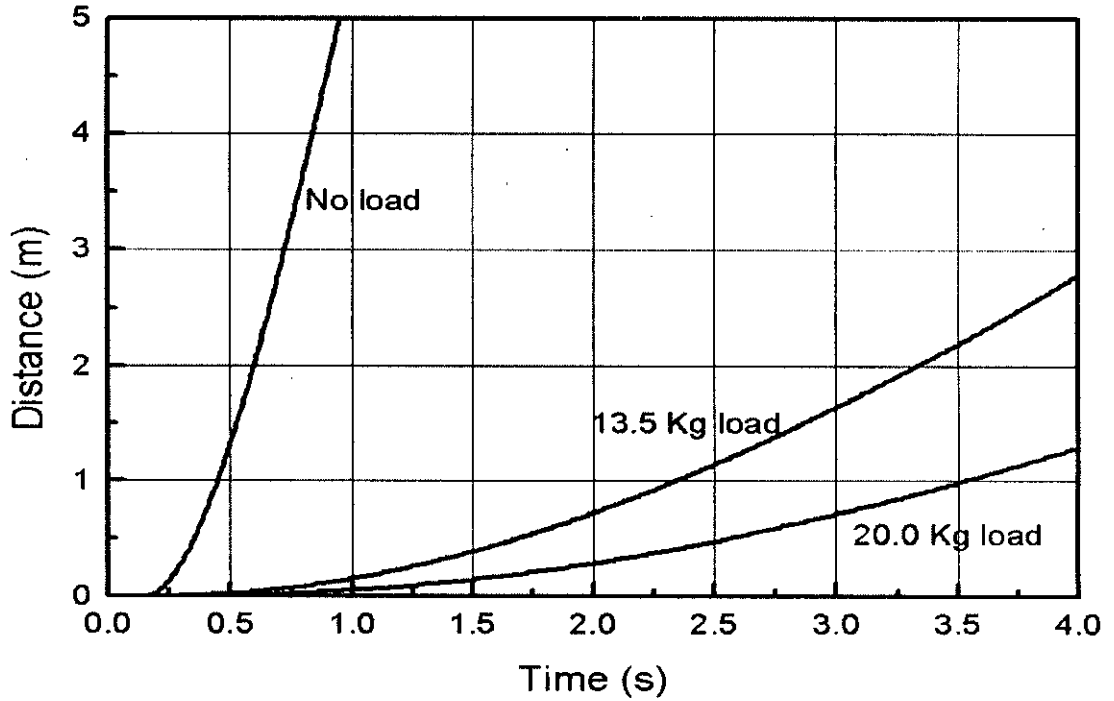


Fig. 5.35. Effect of load on motor traverse at very early stage of motion (100% duty cycle at right motor and 85% duty cycle at the left).

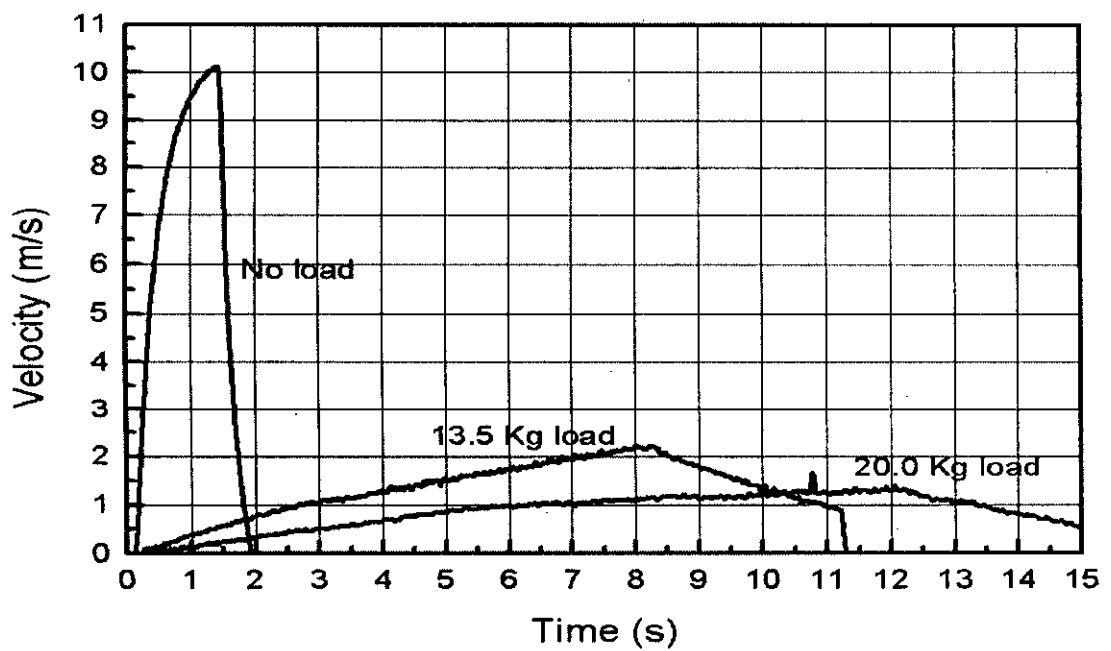


Fig. 5.36. Effect of load on motor speed (100% duty cycle at right motor and 85% duty cycle at the left).

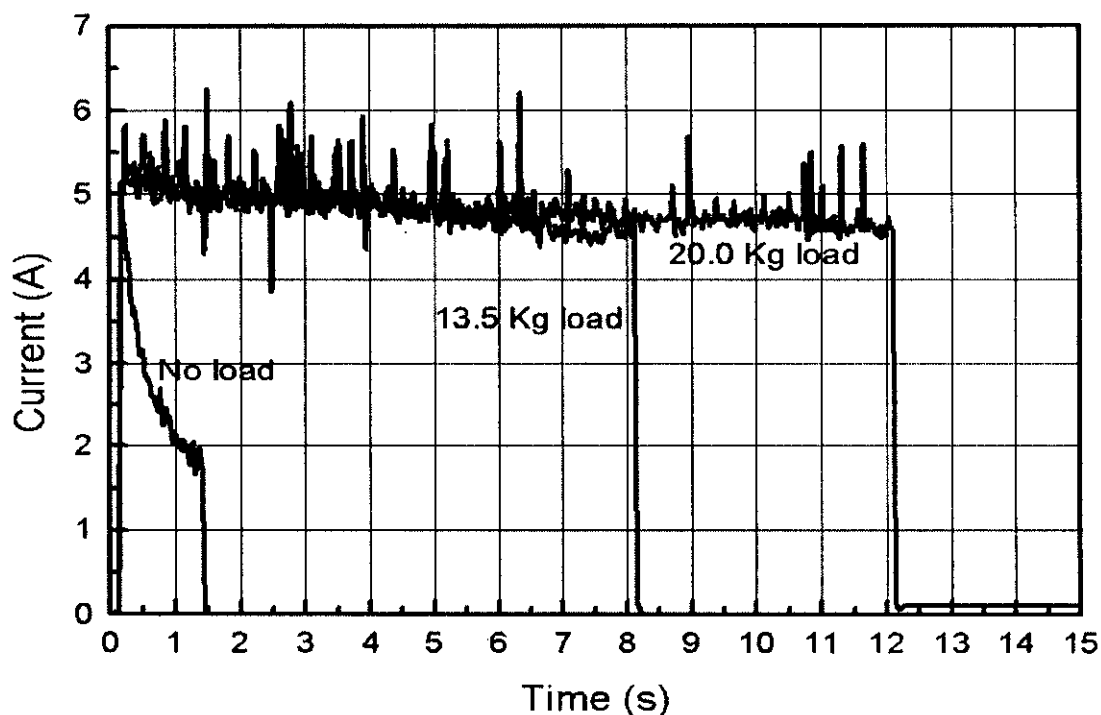


Fig. 5.37. Effect of load on motor current (100% duty cycle at right motor and 85% duty cycle at the left).

Effect of dynamic braking is demonstrated in Fig. 5.38. Dynamic braking is achieved by shorting the motor terminals using SPDT relay controlled by microcontroller. Without the braking motors took longer time to stop, but first stoppage is obtained in case of dynamic braking. Dynamic braking does not employ mechanical friction braking, and therefore does not stop the motor instantly. However, in case of lighter load it is a simple way of stopping the motor which utilizes the back emf of rotating motor and at higher speed the effect is higher.



## 5.2 Conclusions

The conclusions of the present study are as follows:

1. Variation of pulse with modulation (PWM) is an effective mean to control the speed of motor. Hence, PWM can be experimentally varied to obtain its optimum value for straight motion.
2. Loaded motor takes more time to start, achieves lower acceleration and requires longer braking distance.
3. Motor current is high at the very early stage of robot motion with its maximum value just at the point of initiation of motion and motor currents decrease with increase in the robot speed.
4. Dynamic braking is effective in stopping a robot without employing a mechanical friction brake.

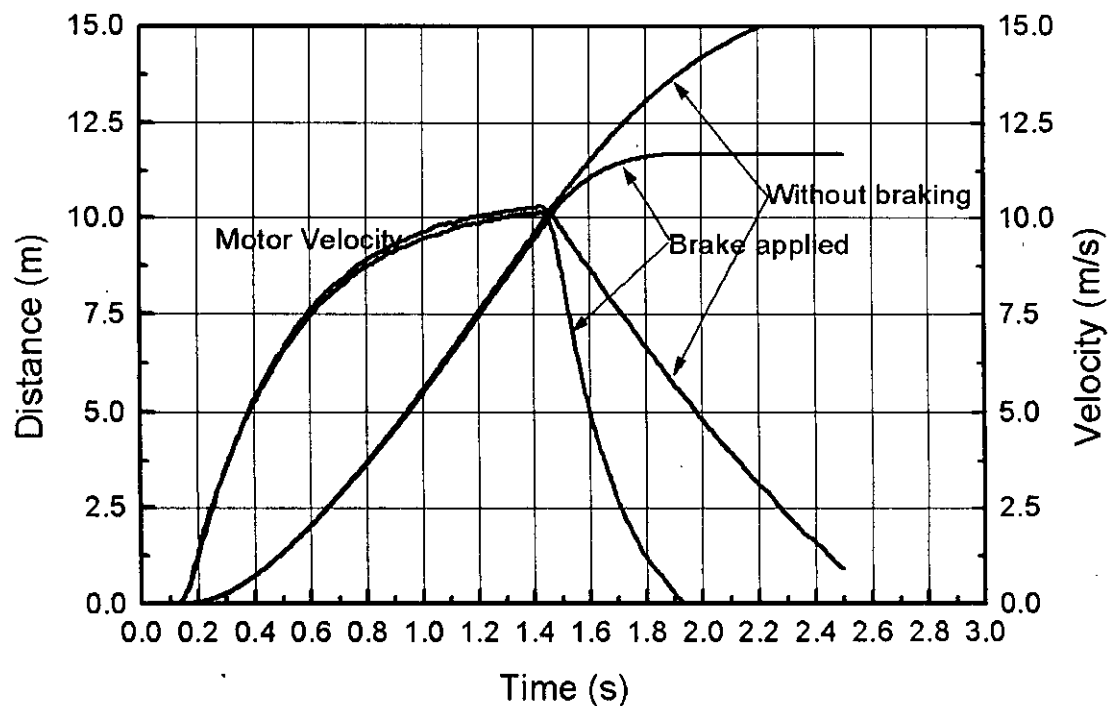


Fig. 5.38. Effect of braking on motor traverse (100% duty cycle at right motor and 85% duty cycle at the left).

### **5.3 Scope of Further Works**

1. Steering of the robot using different pulse width modulation (PWM) to provide synchronized control of motor wheel speed.
2. Optimum value of PWM to achieve a desired motion of a robot.

## References

- [1] Feng, D. and Krogh, BH (2007), Dynamic Steering Control of Conventionally Steered Mobile Robots., pp. 699-721, J. Robotic System.
- [2] Mellodge, P (2002), “ Feedback Control for a Path Following Robotic Car”, M.S. Thesis, Virginia Tech, USA.
- [3] Moret, EN (2003), “Dynamic Modeling and Control of a Car-Like Robot”, M.S. Thesis, Virginia Tech, USA.
- [4] Angeles, J. (2007), Fundamentals of Robotic Mechanical Systems Theory, Methods, and Algorithms, Springer.
- [5] Siciliano, B and Khatib, O (Eds.) (2008), Springer Handbook of Robotics, Springer-Verlag.
- [6] Jone, JL and Flynn, AM (1993), Mobile Robots: Inspiration to Implementation, AK Peters.
- [7] Polka, D (2003), Motors and Drives A Practical Technology Guide, ISA – The Instrumentation, Systems, and Automation Society.
- [8] Ge, S S and Lewis, FL (2006), Autonomous Mobile Robots Sensing, Control, Decision Making and Applications, Taylor & Francis Group, LLC.
- [9] Bräunl , T (2006), Embedded Robotics Mobile Robot Design and Applications with Embedded Systems, Springer-Verlag.
- [10] Siegwart, R and Nourbakhsh, IR (2004), Introduction to Autonomous Mobile Robots, Massachusetts Institute of Technology.
- [11] Iovine, J (2004), PIC Robotics, McGraw-Hill.

[12] Oxford.(2000), The Cutting Edge: An Encyclopedia of Advanced Technology, Oxford.

[13] McLomb and Pedko(2006), Robot Builders Bonanza, McGrawhill.

[14] Luger.G.F (2002), Artificial Intelligence, Addison Wesley.

# Appendix A

## PIC18F452 (28/40-pin High Performance, Enhanced FLASH Microcontrollers with 10-Bit A/D)

### DEVICE OVERVIEW

This document contains device-specific information for the following devices. This family of devices offers the advantages of all PIC18 microcontrollers – namely, high computational performance at an economical price – with the addition of high endurance, Enhanced Flash program memory. In addition to these features, the PIC18F252/452 family introduces design enhancements that make these microcontrollers a logical choice for many high-performance, power sensitive applications.

### High Performance RISC CPU

- C compiler optimized architecture/instruction set
- Linear program memory addressing to 32 Kbytes
- Linear data memory addressing to 1.5 Kbytes
- Up to 10 MIPS operation:
  - DC - 40 MHz osc./clock input
  - 4 MHz - 10 MHz osc./clock input with PLL active
- 16-bit wide instructions, 8-bit wide data path
- Priority levels for interrupts
- 8 x 8 Single Cycle Hardware Multiplier

### Peripheral Features

- High current sink/source 25 mA/25 mA
- Three external interrupt pins
- Timer0 module: 8-bit/16-bit timer/counter with 8-bit programmable prescaler
- Timer1 module: 16-bit timer/counter
- Timer2 module: 8-bit timer/counter with 8-bit period register (time-base for PWM)
- Timer3 module: 16-bit timer/counter
- Secondary oscillator clock option - Timer1/Timer3
- Two Capture/Compare/PWM (CCP) modules. CCP pins that can be configured as:
  - Capture input: capture is 16-bit, max. resolution 6.25 ns (TCY/16)
  - Compare is 16-bit, max. resolution 100 ns (TCY)
  - PWM output: PWM resolution is 1- to 10-bit, max. PWM freq. @: 8-bit resolution = 156 kHz, 10-bit resolution = 39 kHz
- Master Synchronous Serial Port (MSSP) module, Two modes of operation:
  - 3-wire SPI™ (supports all 4 SPI modes)
  - I2C™ Master and Slave mode
- Addressable USART module:
  - Supports RS-485 and RS-232
- Parallel Slave Port (PSP) module

### Analog Features

- Compatible 10-bit Analog-to-Digital Converter module (A/D) with:
  - Fast sampling rate
  - Conversion available during SLEEP
  - Linearity  $\pm 1$  LSB
- Programmable Low Voltage Detection (PLVD)
  - Supports interrupt on-Low Voltage Detection
- Programmable Brown-out Reset (BOR)

### Special Microcontroller Features

- 100,000 erase/write cycle Enhanced FLASH program memory typical
- 1,000,000 erase/write cycle Data EEPROM memory
- FLASH/Data EEPROM Retention: > 40 years
- Self-reprogrammable under software control
- Power-on Reset (POR), Power-up Timer (PWRT) and Oscillator Start-up Timer (OST)
- Watchdog Timer (WDT) with its own On-Chip RC Oscillator for reliable operation
- Programmable code protection
- Power saving SLEEP mode
- Selectable oscillator options including:
  - 4X Phase Lock Loop (of primary oscillator)
  - Secondary Oscillator (32 kHz) clock input
- Single supply 5V In-Circuit Serial Programming™ (ICSP™) via two pins
- In-Circuit Debug (ICD) via two pins

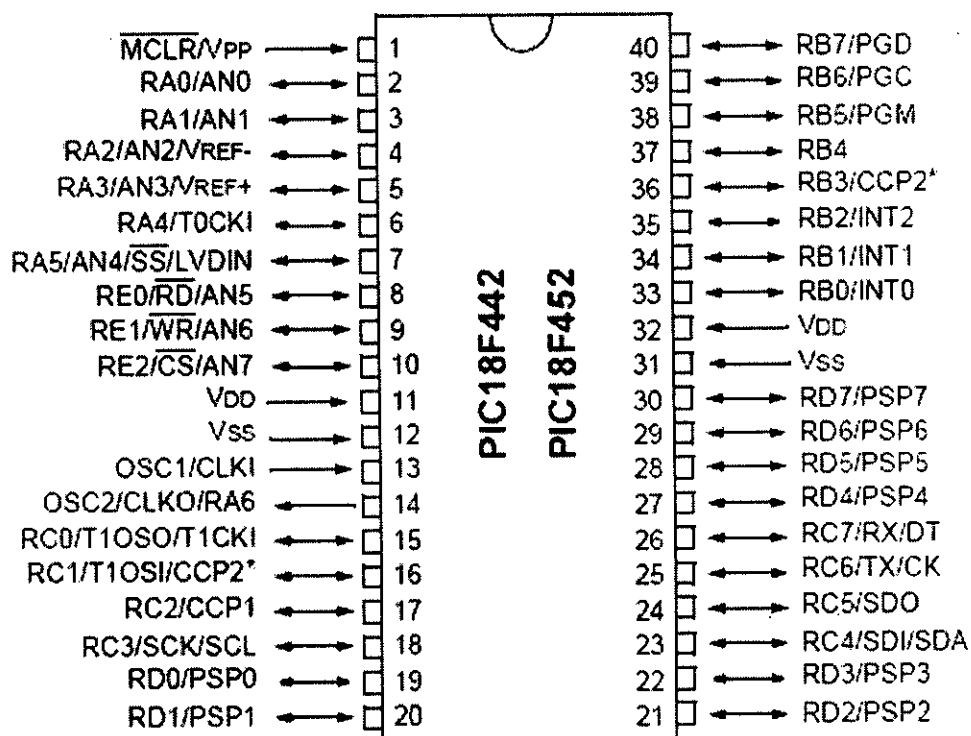
### CMOS Technology

- Low power, high speed FLASH/EEPROM technology
- Fully static design
- Wide operating voltage range (2.0V to 5.5V)
- Industrial and Extended temperature ranges
- Low power consumption:

### DEVICE FEATURES

Features	PIC18F242	PIC18F252	PIC18F442	PIC18F452
Operating Frequency	DC - 40 MHz	DC - 40 MHz	DC - 40 MHz	DC - 40 MHz
Program Memory (Bytes)	16K	32K	16K	32K
Program Memory (Instructions)	8192	16384	8192	16384
Data Memory (Bytes)	768	1536	768	1536
Data EEPROM Memory (Bytes)	256	256	256	256
Interrupt Sources	17	17	18	18
I/O Ports	Ports A, B, C	Ports A, B, C	Ports A, B, C, D, E	Ports A, B, C, D, E
Timers	4	4	4	4
Capture/Compare/PWM Modules	2	2	2	2
Serial Communications	MSSP, Addressable USART	MSSP, Addressable USART	MSSP, Addressable USART	MSSP, Addressable USART
Parallel Communications	—	—	PSP	PSP
10-bit Analog-to-Digital Module	5 input channels	5 input channels	8 input channels	8 input channels
RESETS (and Delays)	POR, BOR, RESET Instruction, Stack Full, Stack Underflow (PWRT, OST)	POR, BOR, RESET Instruction, Stack Full, Stack Underflow (PWRT, OST)	POR, BOR, RESET Instruction, Stack Full, Stack Underflow (PWRT, OST)	POR, BOR, RESET Instruction, Stack Full, Stack Underflow (PWRT, OST)
Programmable Low Voltage Detect	Yes	Yes	Yes	Yes
Programmable Brown-out Reset	Yes	Yes	Yes	Yes
Instruction Set	75 Instructions	75 Instructions	75 Instructions	75 Instructions
Packages	28-pin DIP 28-pin SOIC	28-pin DIP 28-pin SOIC	40-pin DIP 44-pin PLCC 44-pin TQFP	40-pin DIP 44-pin PLCC 44-pin TQFP

## PIC 18F452 Pin Diagram



## Appendix B

### PIC18F2550 (28/40-Pin, High-Performance, Enhanced Flash, USB Microcontrollers with nanoWatt Technology)

#### 1.0 DEVICE OVERVIEW

This document contains device-specific information for the following devices. This family of devices offers the advantages of all PIC18 microcontrollers – namely, high computational performance at an economical price – with the addition of high endurance, Enhanced Flash program memory. In addition to these features, the PIC18F2455/2550 family introduces design enhancements that make these microcontrollers a logical choice for many high-performance, power sensitive applications.

#### 1.1 New Core Features

1.1.1 nanoWatt TECHNOLOGY .All of the devices in the PIC18F2455/2550 family incorporate a range of features that can significantly reduce power consumption during operation. Key items include:

- **Alternate Run Modes:** By clocking the controller from the Timer1 source or the internal oscillator block, power consumption during code execution can be reduced by as much as 90%.
- **Multiple Idle Modes:** The controller can also run with its CPU core disabled but the peripherals still active. In these states, power consumption can be reduced even further, to as little as 4% of normal operation requirements.
- **On-the-Fly Mode Switching:** The power-managed modes are invoked by user code during operation, allowing the user to incorporate power-saving ideas into their application's software design.
- **Low Consumption in Key Modules:** The power requirements for both Timer1 and the Watchdog Timer are minimized. “**Electrical Characteristics**” for values.

1.1.2 **UNIVERSAL SERIAL BUS (USB)** Devices in the PIC18F2455/2550/4455/4550 family incorporate a fully featured Universal Serial Bus communications module that is compliant with the USB Specification Revision 2.0. The module supports both low-speed and full-speed communication for all supported data transfer types. It also incorporates its own on-chip transceiver and 3.3V regulator and supports the use of external transceivers and voltage regulators.

#### 1.1.3 Multiple Oscillator Options And Features

All of the devices in the PIC18F2455/2550/4455/4550 family offer twelve different oscillator options, allowing users a wide range of choices in developing application hardware. These include:

- Four Crystal modes using crystals or ceramic resonators.
- Four External Clock modes, offering the option of using two pins (oscillator input and a divide-by-4 clock output) or one pin (oscillator input, with the second pin reassigned as general I/O).
- An internal oscillator block which provides an 8 MHz clock ( $\pm 2\%$  accuracy) and an INTRC source (approximately 31 kHz, stable over temperature and VDD), as well as a range of 6 user-selectable clock frequencies, between 125 kHz to 4 MHz, for a total of 8 clock frequencies. This option frees an oscillator pin for use as an additional general purpose I/O.



- A Phase Lock Loop (PLL) frequency multiplier, available to both the High-Speed Crystal and External Oscillator modes, which allows a wide range of clock speeds from 4 MHz to 48 MHz.
- Asynchronous dual clock operation, allowing the USB module to run from a high-frequency oscillator while the rest of the microcontroller is clocked from an internal low-power oscillator. Besides its availability as a clock source, the internal oscillator block provides a stable reference source that gives the family additional features for robust Operation:

- **Fail-Safe Clock Monitor:** This option constantly monitors the main clock source against a reference signal provided by the internal oscillator. If a clock failure occurs, the controller is switched to the internal oscillator block, allowing for continued low-speed operation or a safe application shutdown.
  - **Two-Speed Start-up:** This option allows the internal oscillator to serve as the clock source from Power-on Reset, or wake-up from Sleep mode, until the primary clock source is available.
- PIC18F2550 • PIC18LF2550

### 1.2 Other Special Features

- **Memory Endurance:** The Enhanced Flash cells for both program memory and data EEPROM are rated to last for any thousands of erase/write cycles – up to 100,000 for program memory and 1,000,000 for EEPROM. Data retention without refresh is conservatively estimated to be greater than 40 years.
- **Self-Programmability:** These devices can write to their own program memory spaces under internal software control. By using a bootloader routine, located in the protected Boot Block at the top of program memory, it becomes possible to create an application that can update itself in the field.
- **Extended Instruction Set:** The PIC18F2455/2550/4455/4550 family introduces an optional extension to the PIC18 instruction set, which adds 8 new instructions and an Indexed Literal Offset Addressing mode. This extension, enabled as a device configuration option, has been specifically designed to optimize re-entrant application code originally developed in high-level languages such as C.
- **Enhanced CCP Module:** In PWM mode, this module provides 1, 2 or 4 modulated outputs for controlling half-bridge and full-bridge drivers. Other features include auto-shutdown for disabling PWM outputs on interrupt or other select conditions and auto-restart to reactivate outputs once the condition has cleared.
- **Enhanced Addressable USART:** This serial communication module is capable of standard RS-232 operation and provides support for the LIN bus protocol. Other enhancements include Automatic Baud Rate Detection and a 16-bit Baud Rate Generator for improved resolution. When the microcontroller is using the internal oscillator block, the EUSART provides stable operation for applications that talk to the outside world without using an external crystal (or its accompanying power requirement).
- **10-Bit A/D Converter:** This module incorporates programmable acquisition time, allowing for a channel to be selected and a conversion to be initiated, without waiting for a sampling period and thus, reducing code overhead.
- **Dedicated ICD/ICSP Port:** These devices introduce the use of debugger and programming pins that are not multiplexed with other microcontroller features. Offered as an option in select packages, this feature allows users to develop I/O intensive applications while retaining the ability to program and debug in the circuit.

### 1.3 Details on Individual Family Members

Devices in the PIC18F2455/2550/4455/4550 family are available in 28-pin and 40/44-pin packages. The devices are differentiated from each other in six ways:

1. Flash program memory (24 Kbytes for PIC18FX455 devices, 32 Kbytes for PIC18FX550).
2. A/D channels (10 for 28-pin devices, 13 for 40/44-pin devices).
3. I/O ports (3 bidirectional ports and 1 input only port on 28-pin devices, 5 bidirectional ports on 40/44-pin devices).

4. CCP and Enhanced CCP implementation (28-pin devices have two standard CCP modules, 40/44-pin devices have one standard CCP module and one ECCP module).
5. Streaming Parallel Port (present only on 40/44-pin devices).

#### **Universal Serial Bus Features**

- USB V2.0 Compliant
- Low Speed (1.5 Mb/s) and Full Speed (12 Mb/s)
- Supports Control, Interrupt, Isochronous and Bulk Transfers
- Supports up to 32 Endpoints (16 bidirectional)
- 1-Kbyte Dual Access RAM for USB
- On-Chip USB Transceiver with On-Chip Voltage Regulator
- Interface for Off-Chip USB Transceiver
- Streaming Parallel Port (SPP) for USB streaming transfers (40/44-pin devices only)

#### **Power-Managed Modes**

- Run: CPU on, peripherals on
- Idle: CPU off, peripherals on
- Sleep: CPU off, peripherals off
- Idle mode currents down to 5.8
- Sleep mode currents down to 0.1
- Two-Speed Oscillator Start-up

#### **Flexible Oscillator Structure**

- Four Crystal modes, including High Precision PLL for USB
- Two External Clock modes, up to 48 MHz • Internal Oscillator Block:
  - 8 user-selectable frequencies, from 31 kHz to 8 MHz
  - User-tunable to compensate for frequency drift
- Secondary Oscillator using Timer1 @ 32 kHz
- Dual Oscillator options allow microcontroller and USB module to run at different clock speeds
- Fail-Safe Clock Monitor: - Allows for safe shutdown if any clock stops

#### **Peripheral Highlights**

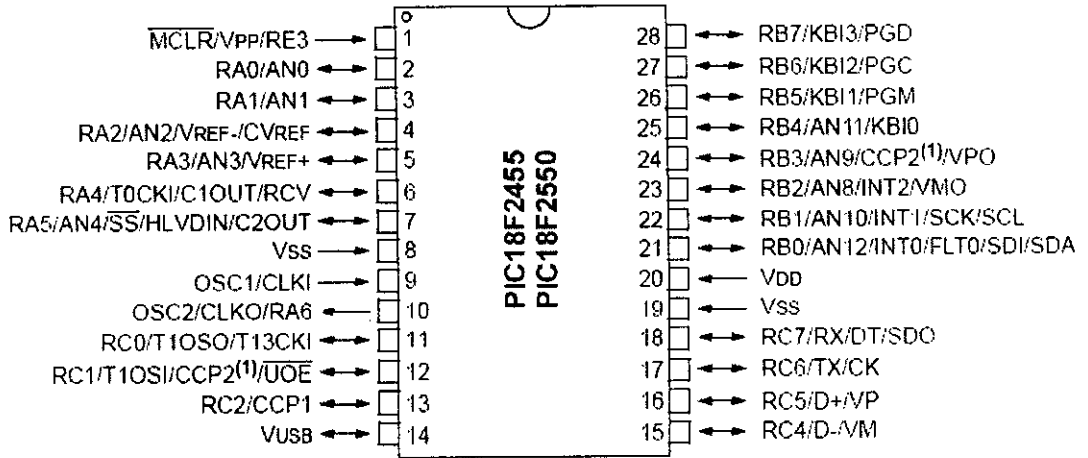
- High-Current Sink/Source: 25 mA/25 mA
- Three External Interrupts
- Four Timer modules (Timer0 to Timer3)
- Up to 2 Capture/Compare/PWM (CCP) modules:
  - Capture is 16-bit, max. resolution 5.2 ns (TCY/16)

- Compare is 16-bit, max. resolution 83.3 ns (TCY)
- PWM output: PWM resolution is 1 to 10-bit
- Enhanced Capture/Compare/PWM (ECCP) module:
  - Multiple output modes
  - Selectable polarity
  - Programmable dead time
  - Auto-shutdown and auto-restart
- Enhanced USART module:
  - LIN bus support
- Master Synchronous Serial Port (MSSP) module supporting 3-wire SPI (all 4 modes) and I2C™ Master and Slave modes
- 10-bit, up to 13-channel Analog-to-Digital Converter module (A/D) with Programmable Acquisition Time
- Dual Analog Comparators with Input Multiplexing

#### **Special Microcontroller Features**

- C Compiler Optimized Architecture with optional Extended Instruction Set
- 100,000 Erase/Write Cycle Enhanced Flash Program Memory typical
- 1,000,000 Erase/Write Cycle Data EEPROM Memory typical
- Flash/Data EEPROM Retention: > 40 years
- Self-Programmable under Software Control
- Priority Levels for Interrupts
- 8 x 8 Single-Cycle Hardware Multiplier
- Extended Watchdog Timer (WDT):
  - Programmable period from 41 ms to 131s
- Programmable Code Protection
- Single-Supply 5V In-Circuit Serial Programming™ (ICSP™) via two pins
- In-Circuit Debug (ICD) via two pins
- Optional dedicated ICD/ICSP port (44-pin devices only)
- Wide Operating Voltage Range (2.0V to 5.5V)

## PIC18F2550 Pin Diagram



## Appendix C

### MAX232 (DUAL DRIVERS / RECEIVERS)

#### DEVICE OVERVIEW

The MAX232 is a dual driver/receiver that includes a capacitive voltage generator to supply TIA/EIA-232-F voltage levels from a single 5-V supply. Each receiver converts TIA/EIA-232-F inputs to 5-V TTL/CMOS levels. These receivers have a typical threshold of 1.3 V, a typical hysteresis of 0.5 V, and can accept  $\pm 30$ -V inputs.

- \_ Meets or Exceeds TIA/EIA-232-F and ITU Recommendation V.28
- \_ Operates From a Single 5-V Power Supply With 1.0- $\mu$ F Charge-Pump Capacitors
- \_ Operates Up To 120 kbit/s
- \_ Two Drivers and Two Receivers
- \_  $\pm 30$ -V Input Levels
- \_ Low Supply Current . . . 8 mA Typical
- \_ ESD Protection Exceeds JESD 22 - 2000-V Human-Body Model (A114-A)
- \_ Upgrade With Improved ESD (15-kV HBM) and 0.1- $\mu$ F Charge-Pump Capacitors is Available With the MAX202
- \_ Applications - TIA/EIA-232-F, Battery-Powered Systems, Terminals, Modems, and Computers

#### Absolute maximum ratings over operating free-air temperature range (unless otherwise noted)†

Input supply voltage range, VCC (see Note 1) . . . . .	-0.3 V to 6V
Positive output supply voltage range, VS+ . . . . .	VCC - 0.3 V to 15 V
Negative output supply voltage range, VS- . . . . .	-0.3 V to -15 V
Input voltage range, VI: Driver . . . . .	-0.3 V to VCC + 0.3 V
Receiver . . . . .	$\pm 30$ V
Output voltage range, VO: T1OUT, T2OUT . . . . .	VS- - 0.3 V to VS+ + 0.3 V
R1OUT, R2OUT . . . . .	-0.3 V to VCC + 0.3 V
Short-circuit duration: T1OUT, T2OUT . . . . .	Unlimited
Package thermal impedance, $\theta_{JA}$ (see Notes 2 and 3):	
D package . . . . .	73°C/W
DW package . . . . .	57°C/W
N package . . . . .	67°C/W
NS package . . . . .	64°C/W

Operating virtual junction temperature,  $T_J$  . . . . . 150°C

Storage temperature range,  $T_{stg}$  . . . . . -65°C to 150°C

† Stresses beyond those listed under "absolute maximum ratings" may cause permanent damage to the device. These are stress ratings only, and functional operation of the device at these or any other conditions beyond those indicated under "recommended operating conditions" is not implied. Exposure to absolute-maximum-rated conditions for extended periods may affect device reliability.

NOTES: 1. All voltages are with respect to network GND.

2. Maximum power dissipation is a function of  $T_J(\max)$ ,  $\theta_{JA}$ , and  $T_A$ . The maximum allowable power dissipation at any allowable ambient temperature is  $PD = (T_J(\max) - T_A)/\theta_{JA}$ . Operating at the absolute maximum  $T_J$  of 150°C can affect reliability.

3. The package thermal impedance is calculated in accordance with JESD 51-7.

## recommended operating conditions

		MIN	NOM	MAX	UNIT
V <sub>CC</sub>	Supply voltage	4.5	5	5.5	V
V <sub>IH</sub>	High-level input voltage (T1IN, T2IN)	2			V
V <sub>IL</sub>	Low-level input voltage (T1IN, T2IN)			0.8	V
R1IN, R2IN	Receiver input voltage			±30	V
T <sub>A</sub>	Operating free-air temperature	MAX232	0	70	°C
		MAX232I	-40	85	

electrical characteristics over recommended ranges of supply voltage and operating free-air temperature (unless otherwise noted) (see Note 4 and Figure 4)

PARAMETER		TEST CONDITIONS	MIN	TYP†	MAX	UNIT
I <sub>CC</sub>	Supply current	V <sub>CC</sub> = 5.5 V, All outputs open, T <sub>A</sub> = 25°C		8	10	mA

† All typical values are at V<sub>CC</sub> = 5 V and T<sub>A</sub> = 25°C.

NOTE 4: Test conditions are C1-C4 = 1 μF at V<sub>CC</sub> = 5 V ± 0.5 V.

## DRIVER SECTION

electrical characteristics over recommended ranges of supply voltage and operating free-air temperature range (see Note 4)

PARAMETER		TEST CONDITIONS	MIN	TYP†	MAX	UNIT
V <sub>OH</sub>	High-level output voltage	T1OUT, T2OUT R <sub>L</sub> = 3 kΩ to GND	5	7		V
V <sub>OL</sub>	Low-level output voltage‡	T1OUT, T2OUT R <sub>L</sub> = 3 kΩ to GND		-7	-5	V
r <sub>o</sub>	Output resistance	T1OUT, T2OUT V <sub>S+</sub> = V <sub>S-</sub> = 0, V <sub>O</sub> = ±2 V	300			Ω
I <sub>OS</sub> §	Short-circuit output current	T1OUT, T2OUT V <sub>CC</sub> = 5.5 V, V <sub>O</sub> = 0		±10		mA
I <sub>IS</sub>	Short-circuit input current	T1IN, T2IN V <sub>I</sub> = 0			200	μA

† All typical values are at V<sub>CC</sub> = 5 V, T<sub>A</sub> = 25°C

‡ The algebraic convention, in which the least-positive (most negative) value is designated minimum, is used in this data sheet for logic voltage levels only.

§ Not more than one output should be shorted at a time.

NOTE 4: Test conditions are C1-C4 = 1 μF at V<sub>CC</sub> = 5 V ± 0.5 V.

switching characteristics, V<sub>CC</sub> = 5 V, T<sub>A</sub> = 25°C (see Note 4)

PARAMETER		TEST CONDITIONS	MIN	TYP	MAX	UNIT
SR	Driver slew rate	R <sub>L</sub> = 3 kΩ to 7 kΩ, See Figure 2			30	V/μs
SR(I)	Driver transition region slew rate	See Figure 3		3		V/μs
	Data rate	One TOUT switching		120		kbit/s

NOTE 4: Test conditions are C1-C4 = 1 μF at V<sub>CC</sub> = 5 V ± 0.5 V.

## RECEIVER SECTION

electrical characteristics over recommended ranges of supply voltage and operating free-air temperature range (see Note 4)

PARAMETER		TEST CONDITIONS		MIN	TYP†	MAX	UNIT
$V_{OH}$	High-level output voltage	R1OUT, R2OUT	$I_{OH} = -1 \text{ mA}$	3.5			V
$V_{OL}$	Low-level output voltage‡	R1OUT, R2OUT	$I_{OL} = 3.2 \text{ mA}$			0.4	V
$V_{IT+}$	Receiver positive-going input threshold voltage	R1IN, R2IN	$V_{CC} = 5 \text{ V}$ , $T_A = 25^\circ\text{C}$		1.7	2.4	V
$V_{IT-}$	Receiver negative-going input threshold voltage	R1IN, R2IN	$V_{CC} = 5 \text{ V}$ , $T_A = 25^\circ\text{C}$	0.8	1.2		V
$V_{hys}$	Input hysteresis voltage	R1IN, R2IN	$V_{CC} = 5 \text{ V}$	0.2	0.5	1	V
$R_i$	Receiver input resistance	R1IN, R2IN	$V_{CC} = 5$ , $T_A = 25^\circ\text{C}$	3	5	7	k $\Omega$

† All typical values are at  $V_{CC} = 5 \text{ V}$ ,  $T_A = 25^\circ\text{C}$ .

‡ The algebraic convention, in which the least-positive (most negative) value is designated minimum, is used in this data sheet for logic voltage levels only.

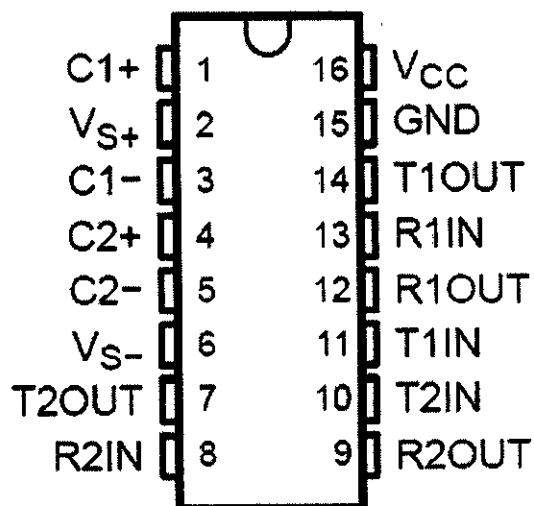
NOTE 4: Test conditions are C1-C4 = 1  $\mu\text{F}$  at  $V_{CC} = 5 \text{ V} \pm 0.5 \text{ V}$ .

switching characteristics,  $V_{CC} = 5 \text{ V}$ ,  $T_A = 25^\circ\text{C}$  (see Note 4 and Figure 1)

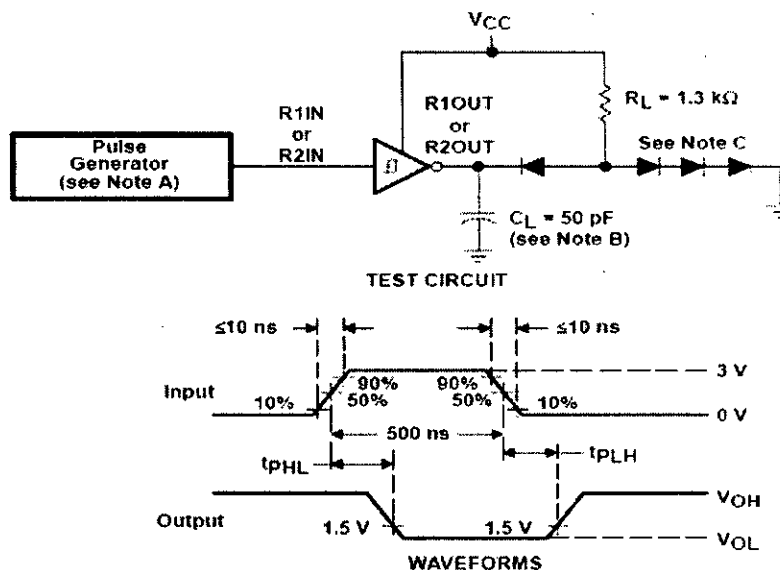
PARAMETER		TYP	UNIT
$t_{PLH(R)}$	Receiver propagation delay time, low- to high-level output	500	ns
$t_{PHL(R)}$	Receiver propagation delay time, high- to low-level output	500	ns

NOTE 4: Test conditions are C1-C4 = 1  $\mu\text{F}$  at  $V_{CC} = 5 \text{ V} \pm 0.5 \text{ V}$ .

### MAX232 . . . D, DW, N, OR NS PACKAGE (TOP VIEW)

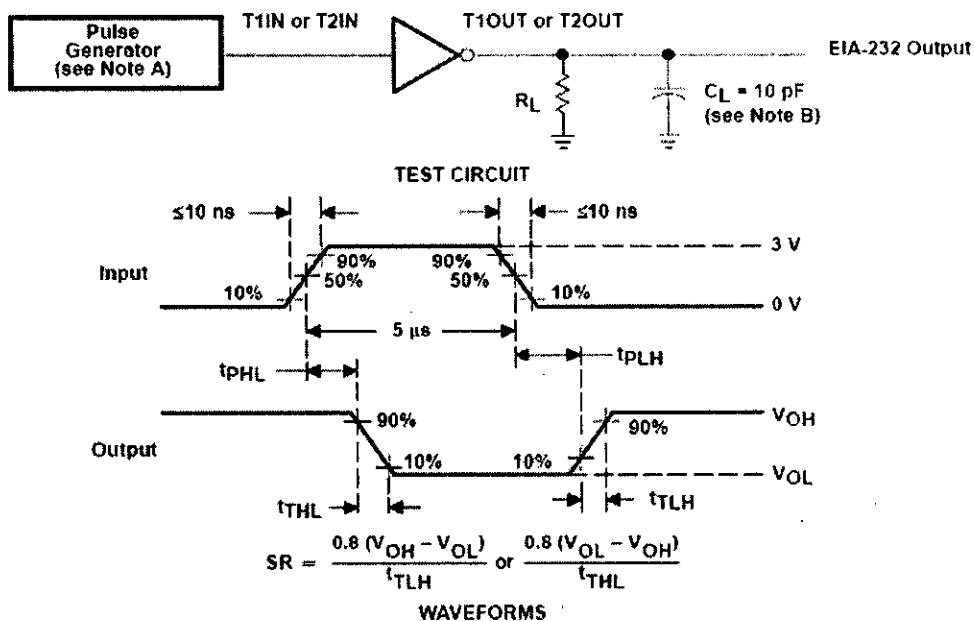


## PARAMETER MEASUREMENT INFORMATION



- NOTES: A. The pulse generator has the following characteristics:  $Z_0 = 50 \Omega$ , duty cycle  $\leq 50\%$ .  
 B.  $C_L$  includes probe and jig capacitance.  
 C. All diodes are 1N3064 or equivalent.

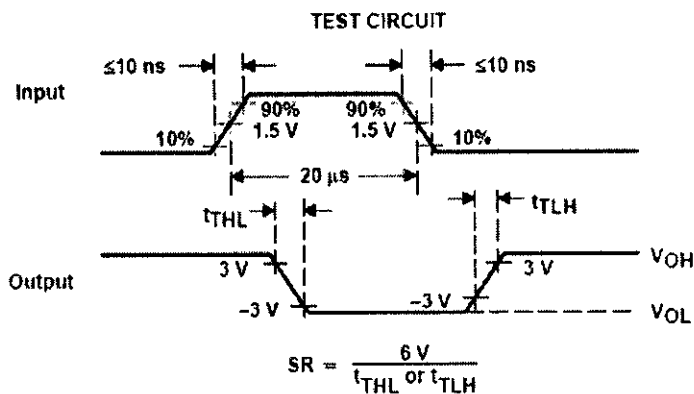
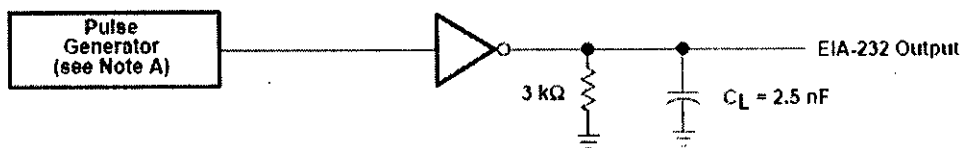
Figure 1. Receiver Test Circuit and Waveforms for  $t_{PHL}$  and  $t_{PLH}$  Measurements



- NOTES: A. The pulse generator has the following characteristics:  $Z_0 = 50 \Omega$ , duty cycle  $\leq 50\%$ .  
 B.  $C_L$  includes probe and jig capacitance.

Figure 2. Driver Test Circuit and Waveforms for  $t_{PHL}$  and  $t_{PLH}$  Measurements (6- $\mu$ s Input)

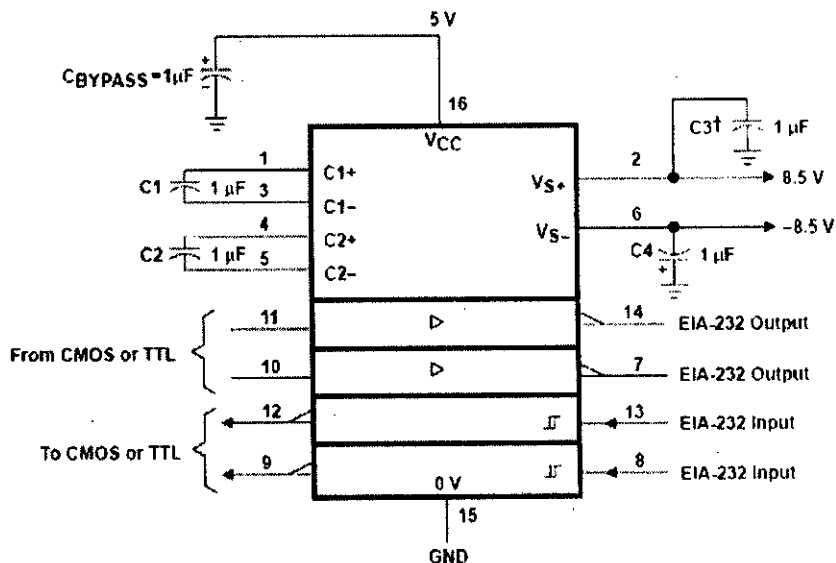




NOTE A: The pulse generator has the following characteristics:  $Z_0 = 50 \Omega$ , duty cycle  $\leq 50\%$ .

Figure 3. Test Circuit and Waveforms for  $t_{THL}$  and  $t_{TLH}$  Measurements (20- $\mu$ s Input)

**APPLICATION INFORMATION**



† C3 can be connected to VCC or GND.

NOTES: A. Resistor values shown are nominal.

B. Nonpolarized ceramic capacitors are acceptable. If polarized tantalum or electrolytic capacitors are used, they should be connected as shown. In addition to the 1- $\mu$ F capacitors shown, the MAX202 can operate with 0.1- $\mu$ F capacitors

Figure 4. Typical Operating Circuit

68290/106289



## Appendix D

### USART Transmission and Receiving Block Diagrams

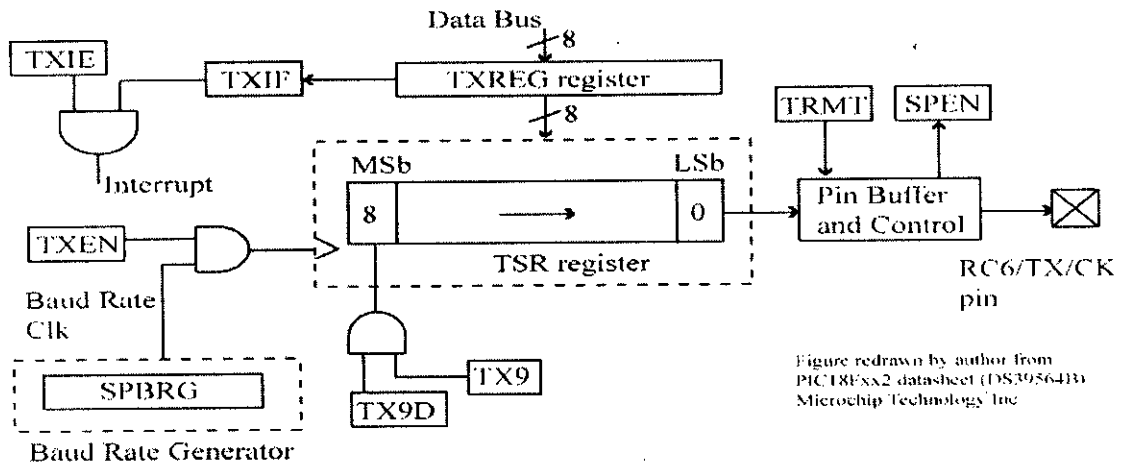


Fig. D.1 USART transmission block diagram

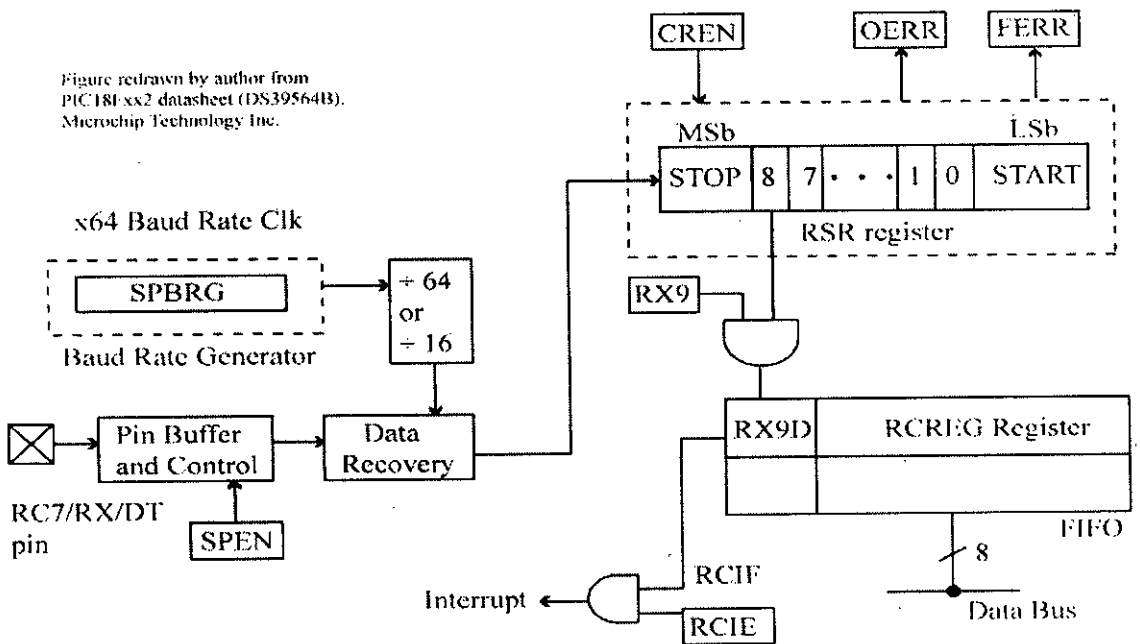


Fig. D.2 USART receiver block diagram.